SPIKES FOR THE GIERER-MEINHARDT SYSTEM WITH DISCONTINUOUS DIFFUSION COEFFICIENTS

JUNCHENG WEI AND MATTHIAS WINTER

Abstract. We rigorously prove results on spiky patterns for the Gierer-Meinhardt system [8] with a jump discontinuity in the diffusion coefficient of the inhibitor. Using numerical computations in combination with a Turing-type instability analysis, this system has been investigated by Benson, Maini and Sherratt [1], [3], [11].

Firstly, we show the existence of an interior spike located away from the jump discontinuity, deriving a necessary condition for the position of the spike. In particular we show that the spike is located in one-and-only-one of the two subintervals created by the jump discontinuity of the inhibitor diffusivity. This **localization principle** for a spike is a **new effect** which does not occur for homogeneous diffusion coefficients. Further, we show that this interior spike is stable.

Secondly, we establish the existence of a spike whose distance from the jump discontinuity is of the same order as its spatial extent. The existence of such a **spike near the jump discontinuity** is the second **new effect** presented in this paper.

To derive these new effects in a mathematically rigorous way, we use analytical tools like Liapunov-Schmidt reduction and nonlocal eigenvalue problems which have been developed in our previous work [24].

Finally, we confirm our results by numerical computations for the dynamical behavior of the system. We observe a moving spike which converges to a stationary spike located in the interior of one of the subintervals or near the jump discontinuity.

1991 *Mathematics Subject Classification.* Primary 35B35, 76E30; Secondary 35B40, 76E06.
Key words and phrases. Pattern Formation, Discontinuous diffusion coefficients, Steady states, Stability.

1. Introduction

We consider a two-component reaction-diffusion system for which the first diffusion coefficient is constant (independent of the spatial variable), whereas the second has a jump discontinuity.

The effect most studied for reaction-diffusion systems is the Turing instability [18] which is characterized by the properties that a spatially homogeneous steady state is stable for spatially homogeneous perturbations, but unstable for some inhomogeneous perturbations. The occurrence of unstable inhomogeneous perturbations explains the onset of spatial patterns.

Since the pioneering paper of Turing pattern-forming reaction-diffusion equations have been successfully used to model a huge variety of biological phenomena such as animal skin patterns, wound healing, cancer growth, embryology, spread of epidemic diseases or even genetic signaling pathways. For a survey we refer to Murray's books [14].

While most of these models assume spatially homogeneous conditions (constant coefficients), in many situations considering systems with spatially varying diffusion coefficients is more realistic. This spatial inhomogeneity can be deduced by assuming that a control chemical regulates the diffusion process of the morphogens (chemical concentration fields) in a reaction-diffusion system. One of the simplest inhomogeneities of the diffusion coefficients are jump discontinuities. This is often a good modelling assumption, for example when two different tissues such as cells of different determination meet at a common border. It also plays a role as a caricature model for more complicated inhomogeneities. We expect that many of the phenomena discovered for jump discontinuities occur also in the general case, possibly in a slightly different fashion.

For systems with jump discontinuities of the diffusion coefficients, Turing instabilities have been computed numerically and investigated analytically by Benson, Maini and Sherratt [1], [3], [11], and results on dispersion relations and typical solution profiles have been obtained. In particular, the authors showed that the spatial variation of diffusion coefficients may produce isolated patterns and asymmetric spatially oscillating patterns which are not seen in standard homogeneous Turing systems. Biological applications of these effects include explaining the anterior-posterior asymmetry of skeletal elements in the limbs of vertebrates and experimental results on double anterior limbs [2], [11], [27].

We give a rigorous mathematical proof of the influence of discontinuous diffusion coefficients on the qualitative and quantitative properties of spiky patterns in a reaction-diffusion system.

In particular, in this paper we study the Gierer-Meinhardt system [8], which is one of the most popular Turing systems [18] of activator-inhibitor type. Adapted to our situation, it reads as follows:

$$\begin{cases} a_t = \epsilon^2 a_{xx} - a + \dfrac{a^2}{h}, \\ \tau h_t = (D(x)h_x)_x - h + a^2. \end{cases} \tag{1.1}$$

Note that h acts as an inhibitor to a, whereas a acts as an activator to both a and h. This motivates the name activator-inhibitor system. In this paper, we assume that $0 < \epsilon << 1$, $\tau \geq 0$ are constants and

$$D(x) = \begin{cases} D_1, & -1 < x < x_b, \\ D_2, & x_b < x < 1, \end{cases} \tag{1.2}$$

where $0 < D_1$, $0 < D_2$, and $D_1 \neq D_2$. In Section 6 we set $\tau = 0.1$ and in Section 12 we assume that τ is small enough. We study the equation (1.1) in the interval $(-1, 1)$ with Neumann boundary conditions

$$a_x(-1) = a_x(1) = 0, \quad h_x(-1) = h_x(1) = 0. \tag{1.3}$$

We rigorously prove the existence of two classes of stationary spiky solutions to this system: first an interior spike which is located far away from the jump discontinuity and second a spike whose distance to the jump discontinuity is of the same order as its spatial extent.

A condition for the position of the interior spike will be derived, namely it can be located in one-and-only-one of the two subintervals. This **localization principle** for spikes is a **new effect** which does not occur for homogeneous diffusion coefficients. Further, we investigate the linearized stability of this interior spiky steady state and we prove that it is always stable.

Concerning the spike near the jump discontinuity, we will show that generically there are two possible locations or there is none. Further, our results imply that it occurs preferably if the discontinuity is located near the center of the interval and if the two diffusion constants differ by a substantial amount.

Now we mention some previous works on spiky steady states for the Gierer-Meinhardt system with constant coefficients. Existence and stability of spiky steady states have been studied for 1D in [9] and their instabilities have been investigated in [20]. For 2D the existence and stability of multiple spikes has been investigated in [22], [23], [24].

Works with spatially varying coefficients include [16], [17] where 1D and 2D complex patterns are investigated, [19] where the 1D and 2D motion of a spike and pinning effects are studied and [15] where the varied behavior of traveling pulses is shown.

The structure of the paper is as follows: in Section 2 we provide some preliminaries. In Section 3 we present the main results of the paper. In Section 4 we introduce and analyze a suitable approximate interior spike steady state. In Section 5 we show the existence of a steady state with a spike near the jump in the diffusion coefficient of the inhibitor. In Section 6 we confirm our analytical results by numerical computations. In Section 7 we discuss our results. In Appendix A (Section 8) we introduce and analyze the Green's function. In Appendix B (Section 9) we derive some estimates for the approximate interior spike steady state. In Appendix C (Section 10) we apply the method of Liapunov-Schmidt reduction to the system. In Appendix D (Section 11) we solve the reduced problem. In Appendix E (Section 12) we show the stability of the steady state with an interior spike.

2. Preliminaries

Before stating our main results in Section 3, in this section we introduce some notation and perform some preliminary analysis.

Throughout this paper, we always assume that $\Omega = (-1,1)$. With $L^2(\Omega)$ and $H^2(\Omega)$ we denote the usual Sobolev spaces.

Since we consider (1.1) – (1.3) for a discontinuous diffusion coefficient $D(x)$ of the inhibitor h, which has a jump at a point x_b, the smoothness of h at x_b is lost. More precisely, for classical solutions $D(x)h_x(x)$ is continuous at $x = x_b$ and therefore $h_x(x)$ has a jump discontinuity at $x = x_b$. To account for this jump discontinuity of h the function spaces have to be chosen very carefully.

We assume that

$$(a,h) \in H^2_N(-1,1) \times H^{2,*}_N(-1,1),$$

where

$$H^2_N(-1,1) := \left\{ a \in H^2(-1,1) \,:\, a_x(-1) = a_x(1) = 0 \right\},$$

$$H^{2,*}(-1,1) := \left\{ h \in H^1(-1,1) \,:\, (D(x)h_x)_x \in L^2(-1,1) \right\},$$

$$H_N^{2,*}(-1,1) := \left\{ h \in H^{2,*}(-1,1) \,:\, h_x(-1) = h_x(1) = 0 \right\},$$

endowed with the norm

$$\|(a,h)\|_{2,*}^2 := \|a\|_{H^2(-1,1)}^2 + \|h\|_{2,*}^2, \text{ where } \|h\|_{2,*}^2 := \|h\|_{H^1(-1,1)}^2 + \|(D(x)h_x)_x\|_{L^2(-1,1)}.$$

The variable w denotes the unique homoclinic solution of the following problem:

$$\begin{cases} w'' - w + w^2 = 0 & \text{in } R^1, \\ w > 0, \quad w(0) = \max_{y\in R} w(y), & w(y) \to 0 \text{ as } |y| \to \infty. \end{cases} \tag{2.1}$$

Note that w is an even function and $w'(y) < 0$ if $y > 0$. An explicit representation is

$$w(y) = \frac{3}{2}\cosh^{-2}\frac{y}{2}.$$

We set

$$\rho(y) := \int_0^y w^2(z)\,dz. \tag{2.2}$$

Elementary calculations give

$$\alpha := \int_0^\infty w^2(y)\,dy = \int_0^\infty w(y)\,dy = 3, \quad \int_0^\infty w^3(y)\,dy = 3.6,$$
$$\rho(y) = \frac{9}{2}\tanh\frac{y}{2} - \frac{3}{2}\tanh^3\frac{y}{2}, \quad \int_0^\infty w^3(y)\rho(y)\,dy = \frac{297}{64} = 4.640625,$$
$$\int_0^\infty (w')^2\,dy = \int_0^\infty w^3\,dy - \int_0^\infty w^2\,dy = 0.6. \tag{2.3}$$

To conclude this section, we study a nonlocal linear operator. We first recall the following result.

Theorem 2.1. [21] *Consider the nonlocal eigenvalue problem*

$$L\phi := \Delta\phi - \phi + 2w\phi - \gamma\frac{\int_R w\phi\,dy}{\int_R w^2\,dy}w^2 = \lambda\phi, \quad \phi \in H^1(R). \tag{2.4}$$

(1) If $\gamma < 1$, then there is a positive eigenvalue to (2.4).

(2) If $\gamma > 1$, then for any nonzero eigenvalue λ of (2.4) we have

$$Re(\lambda) \le -c_0 < 0 \quad \textit{for some } c_0 > 0.$$

(3) If $\gamma \ne 1$ and $\lambda = 0$, then

$$\phi = c_0\frac{dw}{dy}$$

for some constant c_0.

The conjugate operator of L under the scalar product in $L^2(R)$ is

$$L^*\psi = \Delta\psi - \psi + 2w\psi - \gamma \frac{\int_R w^2\psi\, dy}{\int_R w^2\, dy} w, \quad H^2(R) \to L^2(R). \tag{2.5}$$

Then we have the following result.

Lemma 2.2. *(Lemma 3.2 of* [25]*.) If $\gamma \neq 1$, then*

$$X_0 := Ker(L^*) = span\left\{ \frac{dw}{dy} \right\}. \tag{2.6}$$

As a consequence, we have

Lemma 2.3. *The operator*

$$L : H^2(R) \to L^2(R),$$

restricted to the spaces

$$L : X_0^\perp \cap H^2(R) \to X_0^\perp \cap L^2(R),$$

where the $X_0^\perp$ denotes the orthogonal projection with respect to the scalar product of $L^2(R)$, is invertible. Moreover, $L^{-1} : X_0^\perp \cap L^2(R) \to X_0^\perp \cap H^2(R)$ is bounded.

Proof: This follows from the Fredholm Alternative Theorem and Lemma 2.2.

□

3. Main Results: interior spike and spike near the jump discontinuity of the diffusion coefficient

We consider the case when the inhibitor diffusivity is discontinuous with a single jump, and derive two types of one-spike steady states:

1. an **interior spike** located far away from the jump discontinuity of the inhibitor diffusivity (see Theorem 3.1). For this interior spike we derive a **new localization principle**, which states that the spike can exist in one-and-only-one of the two sub-intervals divided by the jump discontinuity. Further, we show that this solution is stable (Theorem 3.3).

2. a **spike near the jump discontinuity** whose center has a distance of order ϵ from the jump discontinuity, which means that its distance from the jump discontinuity is of the same order as the spatial extent of the spike (Theorem 3.4).

We re-scale $\Omega_\epsilon = (-\frac{1}{\epsilon}, \frac{1}{\epsilon})$ and define $u(x) \in H^2_\epsilon(\Omega)$ if and only if $u\left(\frac{x}{\epsilon}\right) \in H^2(\Omega_\epsilon)$, where the norm of the former space is defined by the norm of the latter, i.e.

$$\|u\|_{H^2_\epsilon(\Omega)} := \|u(\cdot/\epsilon)\|_{H^2(\Omega_\epsilon)}.$$

In the same way we introduce this re-scaling to the other function spaces introduced at the beginning of the previous section.

Now we state our first main theorem.

Theorem 3.1. *(Existence of an interior-spike solution.) Suppose that the condition*

$$\frac{1}{\theta_1}\tanh\theta_1(1+x_b) > \frac{1}{\theta_2}\tanh\theta_2(1-x_b) \tag{3.1}$$

holds, where $\theta_i = D_i^{-1/2}$. Then there exists a steady state of (1.1) – (1.3) with an interior spike for the activator which is located in the subinterval $(-1, x_b)$. More precisely, we have

$$a_\epsilon(x) \sim \xi_0 w\left(\frac{x-t^\epsilon}{\epsilon}\right) + o(1) \qquad \text{in } H^2_\epsilon(\Omega), \tag{3.2}$$

where $t^\epsilon \to t_0 \in (-1, x_b)$ and $\xi_0/h(t^\epsilon) \to 1$ as $\epsilon \to 0$. The limit position t_0 is given by

$$\frac{1}{\theta_1}\tanh\left(\theta_1(2t_0+1-x_b)\right) = \frac{1}{\theta_2}\tanh\left(\theta_2(1-x_b)\right). \tag{3.3}$$

If (3.1) holds then there do **not exist** *any steady states of (1.1) – (1.3) with an interior spike for the activator in the subinterval $(x_b, 1)$.*

Remark 3.2. *(i) Condition (3.1) of Theorem 3.1 implies that in the case $x_b = 0$, i.e. if the jump discontinuity is located at the center of the interval, there exists a spike in the subinterval with the larger diffusion constant D_1 (and the smaller θ_1) but not in the other subinterval. This follows from the fact that the function $\tanh\alpha/\alpha$ is strictly monotone decreasing for $\alpha > 0$.*

(ii) Condition (3.1) combines the effects of sub-domain size and diffusion constant. Hence the localization effect is due jointly, and favorably, to relatively large subinterval and large diffusion constant.

(iii) Note that existence of a single spike occurs in one-and-only-one of the subintervals.

(iv) The reverse sign of (3.1) does not have to be studied separately. It follows by reflection about the center $x = 0$ of the interval. By this transformation θ_1 and θ_2 are exchanged and the sign of x_b is

reversed. An easy calculation shows that the inequality resulting from this transformation is equivalent to (3.1) with reversed sign.

(v) The **localization principle** *proved in Theorem 3.1 which has been established here for a reaction-diffusion system with a jump discontinuity of the inhibitor diffusivity is expected to play a general role for reaction-diffusion systems with varying diffusion coefficients. We expect that further investigations of this phenomenon in the general context will show important new effects which are not observed in the classical case of Turing systems with constant diffusion coefficients. This should have important implications for the prediction of localization and asymmetry of patterns in many areas of biology.*

We now give a result for the linear stability of the interior spike.

Theorem 3.3. *(Stability of an interior-spike solution.) The interior spike established in Theorem 3.1 is linearly stable.*

In our second main theorem we establish the existence of spikes near the jump discontinuity of the inhibitor diffusivity, more precisely at a distance of order ϵ from this discontinuity.

Theorem 3.4. *(Existence of spikes near the jump discontinuity x_b of the inhibitor diffusivity.)*

(i) If

$$\begin{cases} \theta_1 < \theta_2 \quad \text{and} \\ 0 < \dfrac{\theta_2 \tanh \theta_1 (1+x_b) - \theta_1 \tanh \theta_2 (1-x_b)}{\theta_2 \tanh \theta_1 (1+x_b) + \theta_1 \tanh \theta_2 (1-x_b)} < \dfrac{\theta_2^2 - \theta_1^2}{2\theta_1^2} \dfrac{I(L_0)}{10.8}, \end{cases} \tag{3.4}$$

there exist exactly two spikes near the jump discontinuity x_b. They are given by (3.2) with $t^\epsilon = x_b - \epsilon L$ for two possible values of L which are solutions of (5.7).

(ii) If condition (3.1) holds and $\theta_1 > \theta_2$, or if

$$\begin{cases} \theta_1 < \theta_2 \quad \text{and} \\ \dfrac{\theta_2 \tanh \theta_1 (1+x_b) - \theta_1 \tanh \theta_2 (1-x_b)}{\theta_2 \tanh \theta_1 (1+x_b) + \theta_1 \tanh \theta_2 (1-x_b)} > \dfrac{\theta_2^2 - \theta_1^2}{2\theta_1^2} \dfrac{I(L_0)}{10.8} > 0, \end{cases} \tag{3.5}$$

there is **no** *spike near the jump discontinuity x_b. More precisely, there is no spike given by (3.2) with $|t^\epsilon - x_b| = O(\epsilon)$.*

In Theorem 3.4 we have used

$$I(L) := \int_L^\infty w^3(y)(\rho(y) - \beta)\, dy, \tag{3.6}$$

where

$$\beta = \alpha \frac{\theta_2 \tanh \theta_1 (1 + x_b) - \theta_1 \tanh \theta_2 (1 - x_b)}{\theta_2 \tanh \theta_1 (x_b + 1) + \theta_1 \tanh \theta_2 (1 - x_b)}, \tag{3.7}$$

$\rho(y)$ is given by (2.2), L_0 is uniquely determined by $\rho(L_0) = \beta$, and $\alpha = 3$.

Remark 3.5. *(i) We have the following results for the positions of the two spikes given by Theorem 3.4 (i) with respect to the jump discontinuity:*

both are positive if

$$\frac{\theta_2 \tanh \theta_1 (1 + x_b) - \theta_1 \tanh \theta_2 (1 - x_b)}{\theta_2 \tanh \theta_1 (1 + x_b) + \theta_1 \tanh \theta_2 (1 - x_b)} > 0.4296875 \frac{\theta_2^2 - \theta_1^2}{\theta_2^2 + \theta_1^2};$$

one is positive and the other is negative if

$$0 < \frac{\theta_2 \tanh \theta_1 (1 + x_b) - \theta_1 \tanh \theta_2 (1 - x_b)}{\theta_2 \tanh \theta_1 (1 + x_b) + \theta_1 \tanh \theta_2 (1 - x_b)} < 0.4296875 \frac{\theta_2^2 - \theta_1^2}{\theta_2^2 + \theta_1^2}.$$

Note that positive position ($L > 0$) means that the spike is located to the left of the jump discontinuity, and negative position ($L < 0$) means that it lies to the right of the jump discontinuity.

(ii) We do not prove stability of the spike near the jump. However, our conjecture is that the spike at the left position is unstable and the spike at the right position is stable.

We have the following simple nonexistence result for spikes near the jump discontinuity.

Corollary 3.6. *Suppose that $\theta_1 < \theta_2$ and*

$$\left| \frac{\theta_2 \tanh \theta_1 (1 + x_b) - \theta_1 \tanh \theta_2 (1 - x_b)}{\theta_2 \tanh \theta_1 (1 + x_b) + \theta_1 \tanh \theta_2 (1 - x_b)} \right| > 0.4296875 \frac{\theta_2^2 - \theta_1^2}{2\theta_1^2}.$$

Then there is **no** *spike near the jump discontinuity, i.e. a spike with the center satisfying $|t^\epsilon - x_b| = O(\epsilon)$.*

Remark 3.7. *The criterion given in Corollary 3.6 for nonexistence is satisfied if θ_1 and θ_2 are fixed constants which satisfy $\theta_1 < \theta_2 < 2.37793\, \theta_1$ and the jump location x_b is sufficiently close to +1 or -1. This means that we have non-existence if the diffusion constants are sufficiently close to each other* **and** *the jump discontinuity is located sufficiently close to either end of the interval.*

4. The approximate interior spike

We now construct an approximate steady state of (1.1) – (1.3) which has a spike of the activator $a(x)$ concentrating at a point $t_0 \in (-1,1) \setminus \{x_b\}$. For $t_0 \in (-1,1)$, let $t \in B_{\epsilon^{3/4}}(t_0) := \left\{t \in (-1,1) \,:\, |t-t_0| < \epsilon^{3/4}\right\}$. Set

$$w_0(x) = w\left(\frac{x-t}{\epsilon}\right), \tag{4.1}$$

where $w(y)$ is given by (2.1). Let r_0 be such that

$$r_0 = \frac{1}{10}\left(\min\left(t_0+1,\, 1-t_0\right)\right). \tag{4.2}$$

Introduce a smooth cut-off function $\chi : R \to [0,1]$ such that

$$\chi(x) = 1 \quad \text{for} \quad |x| < 1 \quad \text{and} \quad \chi(x) = 0 \quad \text{for} \quad |x| > 2. \tag{4.3}$$

Setting

$$\tilde{w}_0(x) = w_0(x)\chi\left(\frac{x-t}{r_0}\right), \tag{4.4}$$

then $\tilde{w}_0(x)$ satisfies

$$\epsilon^2 \Delta \tilde{w}_0 - \tilde{w}_0 + \tilde{w}_0^2 + \text{e.s.t.} = 0 \quad \text{in } (-1,1), \quad \tilde{w}_0'(-1) = \tilde{w}_0'(1) = 0, \tag{4.5}$$

where "e.s.t." denotes exponentially small terms. For $t \in (-1,1)$, let

$$\hat{\xi}_0(t) = \frac{1}{G(t,t)}, \tag{4.6}$$

where $G(x,y)$ is the Green's function, defined in (8.1). It can be used to represent a steady state of the second equation of (1.1) and plays a major role throughout the paper. This Green's function will be analyzed in detail in Appendix A. We will mostly drop the argument of $\hat{\xi}_0(t)$ and write $\hat{\xi}_0$ instead. Set

$$\xi_0 := \hat{\xi}_0 \xi_\epsilon, \tag{4.7}$$

where

$$\xi_\epsilon := \left(\epsilon \int_R w^2(z)\, dz\right)^{-1} = \frac{1}{6\epsilon}. \tag{4.8}$$

Then, finally, we choose the first component of our approximate steady state for (1.1) to be

$$w_{\epsilon,t}(x) = \xi_0 \tilde{w}_0(x). \tag{4.9}$$

For a function $A \in L^2(-1,1)$, we define $T[A]$ to be the solution in $H_N^{2,*}(-1,1)$ of

$$(D(x)(T[A])_x)_x - T[A] + A^2 = 0. \tag{4.10}$$

By standard elliptic theory, the solution $T[A]$ is positive and unique.

For $A = w_{\epsilon,t}$, where $t \in B_{\epsilon^{3/4}}(t_0)$, we choose the function $T[A](x)$ to be the second component of our approximate steady state for (1.1).

Some error estimates for the approximate steady state $(w_{\epsilon,t}, T[w_{\epsilon,t}])$ are required. They will be derived in Appendix B and form the basis of the existence proof. In Appendix C we will reduce the problem to finite dimensions by Liapunov-Schmidt reduction. In Appendix D we will solve the resulting finite-dimensional problem.

We now discuss some observations about the limit positions of the interior spike by analyzing (3.3).

For the solution of (3.3) we have $t_0 \to 0$ in either of the limits

(i) $\theta_2 \to \theta_1$ (for $\theta_1 = \text{const.}$) (the system approaches the standard GM system with constant diffusivities).

(ii) $\theta_1 \to 0$ and $\theta_2 \to 0$ (the system approaches the shadow system with $D = \infty$).

The spike connects to the spike in the center of the domain, which is the unique spiky steady state for constant diffusivities or the shadow system.

(iii) In the limit $\theta_2 \to \infty$ (for $\theta_1 = \text{const.}$) we get $t_0 \to (x_b - 1)/2 \in (-1, x_b)$. Note that $-1 < (x_b - 1)/2 < 0$. The spikes moves to the center of the subinterval with finite diffusion constant D_1 of the inhibitor if the other diffusion constant D_2 tends to zero.

(iv) Finally, if θ_1 and θ_2 are such that the inequality (3.1) approaches equality, the limit position t_0 approaches x_b.

Note that we always have $t_0 \geq (x_b - 1)/2$ since otherwise (3.3) can not hold ($t_0 < (x_b - 1)/2$ implies l.h.s. of (3.3) is negative while r.h.s. is positive).

By the above, we observe that we can obtain a single spike steady state centered at any point of the open interval $((x_b - 1)/2, x_b)$ by varying the diffusion constants D_1 and D_2. This is a new effect which does not occur for constant diffusivities, where the interior spike is always located at the center of the interval. This shows that for discontinuous diffusion coefficients asymmetric instead of symmetric spike positions are the commonplace. This has some important consequences for biological applications, e.g. for understanding limb development.

In Appendix E we will show that this interior spike steady state is linearly stable.

It turns out that there are small ($o(1)$) and large ($O(1)$) eigenvalues as $\epsilon \to 0$ which are studied separately. It is easy to see that there are no eigenvalues which tend to infinity – we omit the proof of this statement, see e.g. [24].

For large eigenvalues one has to study nonlocal eigenvalue problems. For small eigenvalues one has to apply a projection to a finite-dimensional space similar to Liapunov-Schmidt reduction.

5. Spike near the jump discontinuity of the inhibitor diffusivity

We prove Theorem 3.4 on the existence of spikes near the jump discontinuity x_b of the inhibitor diffusivity.

Proof of Theorem 3.4: Let

$$a_\epsilon(x) = \xi_0 w\left(\frac{x-t^\epsilon}{\epsilon}\right)\chi\left(\frac{x-t^\epsilon}{\epsilon}\right) + O(\epsilon) \quad \text{in } H^2(\Omega_\epsilon),$$

where t_ϵ is the center of the spike, $x_b - t^\epsilon = \epsilon L$ and ξ_0 is given by (4.7). Then we compute an approximation to the second component $h_\epsilon(x)$. We decompose h_ϵ into two parts:

$$h_\epsilon(x) = \xi_0\left(\epsilon h_1\left(\frac{x-t^\epsilon}{\epsilon}\right) + h_2(x)\right) + O(\epsilon) \quad \text{in } H^{2,*}(\Omega_\epsilon), \tag{5.1}$$

where the inner expansion $h_1(y)$ for $y = (x-t^\epsilon)/\epsilon$ satisfies

$$\begin{cases} (D(t^\epsilon + \epsilon y)h_{1,y}(y))_y + w^2(y) = 0, \\ h_1(0) = 0,\ h_{1,y}(0) = 0 \end{cases} \tag{5.2}$$

and the outer expansion $h_2(x)$ is given by

$$\begin{cases} (D(x)h_{2,x}(x))_x - h_2(x) - \epsilon h_1(x) = 0, \\ h_{2,x}(\pm 1) = -h_{1,y}(\pm\infty). \end{cases} \tag{5.3}$$

Integrating (5.2) yields

$$h_{1,y}(y) = \begin{cases} -\theta_1^2\rho(y), & -\infty < y < L, \\ -\theta_2^2\rho(y), & L < y < \infty, \end{cases} \tag{5.4}$$

where $\theta_i = D_i^{-1/2}$ and $\rho(y)$ has been defined in (2.2).

Recalling from (2.3) that

$$\alpha = \int_0^\infty w^2(z)\,dz = 3$$

we have

$$h_{1,y}(-\infty) = \theta_1^2\alpha, \quad h_{1,y}(\infty) = -\theta_2^2\alpha.$$

Note that (2.3) implies

$$\frac{\int_0^\infty w^3(y)\rho(y)\,dy}{\alpha\int_0^\infty w^3(y)} = 0.4296875.$$

Integrating (5.4) again, we have (up to order $O(\epsilon)$ which is included into the error term in (5.1))

$$\epsilon h_1\left(\frac{x-t^\epsilon}{\epsilon}\right) = \begin{cases} \theta_1^2\alpha(x-x_b), & -1<x<x_b, \\ -\theta_2^2\alpha(x-x_b), & x_b<x<1. \end{cases} \tag{5.5}$$

Hence h_2 satisfies (up to order $O(\epsilon)$ which is included into the error term in (5.1))

$$\begin{cases} (D(x)h_{2,x}(x))_x - h_2(x) - \epsilon h_1(x) = 0, \\ h_{2,x}(-1) = -\theta_1^2\alpha, \quad h_{2,x}(1) = \theta_2^2\alpha. \end{cases} \tag{5.6}$$

Solving (5.6), using (5.5), we get

$$h_2(x) = \begin{cases} -\theta_1^2\alpha(x-x_b) + A\theta_1\dfrac{\cosh\theta_1(x+1)}{\cosh\theta_1(x_b+1)}, & -1<x<x_b, \\ \theta_2^2\alpha(x-x_b) + B\theta_1\dfrac{\cosh\theta_2(x-1)}{\cosh\theta_2(x_b-1)}, & x_b<x<1, \end{cases}$$

Continuity of the function $h_2(x)$ at $x=x_b$ gives $A=B$ and continuity of $D(x)h_{2,x}(x)$ at $x=x_b$ implies

$$0 = D_1h_{2,x}(x_b^-) - D_2h_{2,x}(x_b^+) = A\left(\tanh\theta_1(x_b+1) + \frac{\theta_1}{\theta_2}\tanh\theta_2(1-x_b)\right) - 2\alpha$$

and so we have

$$A = \frac{2\alpha\theta_2}{\theta_2\tanh\theta_1(x_b+1) + \theta_1\tanh\theta_2(1-x_b)}.$$

(Note that (3.1) implies

$$A > \frac{\alpha}{\tanh\theta_1(x_b+1)}.)$$

Hence

$$D_1h_{2,x}(x_b^-) = D_2h_{2,x}(x_b^+) = A\tanh\theta_1(x_b+1) - \alpha = \alpha\frac{\theta_2\tanh\theta_1(x_b+1) - \theta_1\tanh\theta_2(1-x_b)}{\theta_2\tanh\theta_1(x_b+1) + \theta_1\tanh\theta_2(1-x_b)}$$

which implies

$$h_{2,x}(x_b^-) = \theta_1^2\beta, \quad h_{2,x}(x_b^+) = \theta_2^2\beta,$$

where

$$\beta = \alpha \frac{\theta_2 \tanh \theta_1 (x_b + 1) - \theta_1 \tanh \theta_2 (1 - x_b)}{\theta_2 \tanh \theta_1 (x_b + 1) + \theta_1 \tanh \theta_2 (1 - x_b)}.$$

Finally, we apply Liapunov-Schmidt reduction as in Appendix C to reduce the problem to one dimension. Following the argument in Appendix D to solve this reduced problem and determine the position of the spike we get the following solvability condition:

$$\begin{aligned}
0 &= \xi_\epsilon^{-1} \int_{-\infty}^{\infty} w^3(y) h_x(t^\epsilon + \epsilon y)\, dy + O(\epsilon) \\
&= \int_{-\infty}^{\infty} w^3(y)(h_{1,y}(y) + h_{2,x}(t^\epsilon + \epsilon y))\, dy + O(\epsilon) \\
&= \int_{-\infty}^{L} w^3(y)(-\theta_1^2 \rho(y) + h_{2,x}(x_b^-))\, dy + \int_{L}^{\infty} w^3(y)(-\theta_2^2 \rho(y) + h_{2,x}(x_b^+))\, dy + O(\epsilon) \\
&= \theta_1^2 \left(\int_{-\infty}^{L} w^3(y)(-\rho(y) + \beta)\, dy \right) + \theta_2^2 \left(\int_{L}^{\infty} w^3(y)(-\rho(y) + \beta)\, dy \right) + O(\epsilon) \\
&= \theta_1^2 \left(\int_{-\infty}^{\infty} w^3(y)(-\rho(y) + \beta)\, dy - \int_{L}^{\infty} w^3(y)(-\rho(y) + \beta)\, dy \right) + \theta_2^2 \left(\int_{L}^{\infty} w^3(y)(-\rho(y) + \beta)\, dy \right) + O(\epsilon) \\
&= \beta \theta_1^2 \int_{-\infty}^{\infty} w^3(y)\, dy + (\theta_2^2 - \theta_1^2) \int_{L}^{\infty} w^3(y)(-\rho(y) + \beta)\, dy + O(\epsilon)
\end{aligned}$$

since $\rho(y)$ is an odd function.

Hence, for given θ_1, θ_2, β, we need to find L such that

$$\beta \theta_1^2 \int_{-\infty}^{\infty} w^3(y)\, dy + (\theta_2^2 - \theta_1^2) \int_{L}^{\infty} w^3(y)(-\rho(y) + \beta)\, dy = 0. \tag{5.7}$$

We recall and summarize that

$$\beta = \alpha \frac{\theta_2 \tanh \theta_1 (1 + x_b) - \theta_1 \tanh \theta_2 (1 - x_b)}{\theta_2 \tanh \theta_1 (1 + x_b) + \theta_1 \tanh \theta_2 (1 - x_b)}, \quad \alpha = 3, \quad \rho(y) = \int_0^y w^2(z)\, dz = \frac{9}{2} \tanh \frac{y}{2} - \frac{3}{2} \tanh^3 \frac{y}{2}.$$

We now check when condition (5.7) can be satisfied. We need to consider only the case $\beta > 0$ which is equivalent to (3.1). Note that for $\beta = 0$ (5.7) is not possible if $\theta_1 \neq \theta_2$ and so we do not consider that case any further.

The case $\beta < 0$ can be reduced to the case $\beta > 0$ by reflection about the center $x = 0$ of the domain. This can be seen as follows: by this reflection θ_1 and θ_2 are exchanged, x_b, t^ϵ, β all change sign. Note that the order of the locations of the jump discontinuity and the spike are reversed so that the equation $x_b = t^\epsilon + \epsilon y$ with $y = L$ changes to $-x_b = -t^\epsilon + \epsilon y$ with $y = -L$. As a result, (5.7) is transformed to

$$-\beta \theta_2^2 \int_{-\infty}^{\infty} w^3(y)\, dy + (\theta_1^2 - \theta_2^2) \int_{-L}^{\infty} w^3(y)(-\rho(y) + \beta)\, dy = 0$$

which is equivalent to (5.7).

We know from Theorem 3.1 that the interior spike solution must be located to the left of the jump discontinuity. Now we show that generically for the spike near the jump discontinuity there are two possible locations or there is none.

A necessary condition is

$$\theta_1^2 < \theta_2^2.$$

Otherwise (5.7) implies

$$\beta\theta_1^2 \int_{-\infty}^{L} w^3(y)\, dy + \theta_1^2 \int_L^\infty w^3(y)\rho(y)\, dy = \theta_2^2 \int_L^\infty w^3(y)(\rho(y) - \beta)\, dy.$$

If $\theta_1^2 \geq \theta_2^2$ in the last equation we have l.h.s is greater than r.h.s. which gives a contradiction.

We now study (5.7) in detail.

An important observation is that the integrand of

$$\int_L^\infty w^3(y)(-\rho(y) + \beta)\, dy$$

changes sign at $\rho(y) = \beta$.

The function ρ has the following properties:

$$\rho(0) = 0, \quad \rho^{'}(y) = w^2(y) > 0, \quad \rho(-y) = -\rho(y),$$

$$\rho(y) \to \int_0^\infty w^2\, dy = \alpha (= 3) \text{ as } y \to \infty \tag{5.8}$$

and β satisfies the inequality

$$0 < \beta = \alpha \frac{\theta_2 \tanh\theta_1(1 + x_b) - \theta_1 \tanh\theta_2(1 - x_b)}{\theta_2 \tanh\theta_1(x_b + 1) + \theta_1 \tanh\theta_2(1 - x_b)} < \alpha.$$

Thus for all $0 < \beta < \alpha$ there is exactly one positive $y =: L_0 > 0$ such that $\rho(L_0) - \beta = 0$. Further, $\rho(y) - \beta < 0$ if $0 < y < L_0$ and $\rho(y) - \beta > 0$ if $y > L_0$.

To give an explicit formula for L_0, using (2.3) we compute

$$\rho(L_0) = \frac{9}{2} \tanh\frac{L_0}{2} - \frac{3}{2} \tanh^3 \frac{L_0}{2} = \beta.$$

From this equation L_0 can be uniquely calculated.

Recall from (3.6) that for any real number L we have defined

$$I(L) := \int_L^\infty w^3(y)(\rho(y) - \beta)\, dy.$$

Then

(i) $I(L) \to 0$ as $L \to \infty$, $\quad I(L) \to -7.2\beta < 0$ as $L \to -\infty$,

(ii) $I(L)$ achieves its unique maximum among all real L at $L = L_0 > 0$, where $I(L_0) > 0$,

(iii) $I(L)$ is monotone increasing on $(-\infty, L_0)$,

(iv) $I(L)$ is monotone decreasing on (L_0, ∞),

(v) $I(L) = 0$ for a unique $L = L_1 < 0$.

Therefore the equation $I(L) = c$ has

$$\begin{cases} \text{two solutions} & \text{if } 0 < c < I(L_0), \\ \text{one solution} & \text{if } c = I(L_0) \text{ or } -7.2\beta < c \le 0, \\ \text{no solution} & \text{if } c > I(L_0) \text{ or } c \le -7.2\beta. \end{cases} \tag{5.9}$$

Since we assume $\theta_1 < \theta_2$, for (5.7) only the case $c > 0$ is relevant. Combining (5.9) with (5.7) and putting $c = \frac{\theta_2 \tanh \theta_1 (1+x_b) - \theta_1 \tanh \theta_2 (1-x_b)}{\theta_2 \tanh \theta_1 (1+x_b) + \theta_1 \tanh \theta_2 (1-x_b)} \frac{10.8 \cdot 2\theta_1^2}{\theta_2^2 - \theta_1^2}$, we have

(i) two solutions for (5.7) if

$$0 < \frac{\theta_2 \tanh \theta_1 (1 + x_b) - \theta_1 \tanh \theta_2 (1 - x_b)}{\theta_2 \tanh \theta_1 (1 + x_b) + \theta_1 \tanh \theta_2 (1 - x_b)} < \frac{\theta_2^2 - \theta_1^2}{2\theta_1^2} \frac{I(L_0)}{10.8}.$$

(ii) no solution for (5.7) if

$$\frac{\theta_2 \tanh \theta_1 (1 + x_b) - \theta_1 \tanh \theta_2 (1 - x_b)}{\theta_2 \tanh \theta_1 (1 + x_b) + \theta_1 \tanh \theta_2 (1 - x_b)} > \frac{\theta_2^2 - \theta_1^2}{2\theta_1^2} \frac{I(L_0)}{10.8}.$$

The proof of Theorem 3.4 is completed.

□

Proof of Remark 3.5: We compute

$$I(0) = 10.8 \left(0.4296875 - \frac{\theta_2 \tanh \theta_1 (1 + x_b) - \theta_1 \tanh \theta_2 (1 - x_b)}{\theta_2 \tanh \theta_1 (1 + x_b) + \theta_1 \tanh \theta_2 (1 - x_b)} \right).$$

Therefore (5.7) implies that in Case (i) both solutions are positive if $c > I(0)$, which implies

$$\frac{\theta_2 \tanh \theta_1 (1 + x_b) - \theta_1 \tanh \theta_2 (1 - x_b)}{\theta_2 \tanh \theta_1 (1 + x_b) + \theta_1 \tanh \theta_2 (1 - x_b)} > 0.4296875 \frac{\theta_2^2 - \theta_1^2}{\theta_2^2 + \theta_1^2},$$

one is positive, the other negative if $c < I(0)$, which implies

$$0 < \frac{\theta_2 \tanh \theta_1 (1 + x_b) - \theta_1 \tanh \theta_2 (1 - x_b)}{\theta_2 \tanh \theta_1 (1 + x_b) + \theta_1 \tanh \theta_2 (1 - x_b)} < 0.4296875 \frac{\theta_2^2 - \theta_1^2}{\theta_2^2 + \theta_1^2}.$$

□

Proof of Corollary 3.6: We consider the following two limits. As $\beta \to 0$ we have $L_0 \to 0$ and

$$I(L_0) \to \int_0^\infty w^3(y) \rho(y)\, dy = 4.640625.$$

As $\beta \to \alpha = 3$ we have $L_0 \to \infty$ and $I(L_0) \to 0$. For β varying between these two extreme values the change of $I(L_0)$ is strictly monotone.

As a consequence we get $0 \leq I(L_0) \leq 4.640625$ which implies the following necessary condition for existence:

$$0 < \frac{\theta_2 \tanh \theta_1(1+x_b) - \theta_1 \tanh \theta_2(1-x_b)}{\theta_2 \tanh \theta_1(1+x_b) + \theta_1 \tanh \theta_2(1-x_b)} < 0.4296875 \frac{\theta_2^2 - \theta_1^2}{2\theta_1^2}. \tag{5.10}$$

Again, for $\beta < 0$, we can use the reflection argument mentioned before. Then with the assumption $\theta_1 > \theta_2$, we get the formula in Corollary 3.6.

□

Proof of Remark 3.7: There are cases when (5.10) is not true. For example, given θ_1, θ_2 such that

$$0 < \theta_1 < \theta_2 < \left(\frac{2.4296875}{0.4296875}\right)^{1/2} \theta_1 \approx 2.37793\, \theta_1,$$

then

$$0 < 0.4296875 \frac{\theta_2^2 - \theta_1^2}{2\theta_1^2} < 1$$

and so by choosing x_b close enough to 1 or -1 (5.10) fails to hold. So in this case there are no spikes in order ϵ distance from the jump discontinuity. The proof is finished.

□

We now discuss the behavior of spikes near the jump in certain limits.

(i) If $\theta_2 \to \infty$ (and $\theta_1 = \text{const.}$), we have $\beta \to 3$. We can re-write (5.7) as

$$7.2\beta \frac{\theta_1^2}{\theta_2^2 - \theta_1^2} = I(L).$$

Solutions to (5.7) exist iff

$$7.2\beta \frac{\theta_1^2}{\theta_2^2 - \theta_1^2} < I(L_0). \tag{5.11}$$

An asymptotic analysis reveals that

$$e^{-2L_0} \sim c(3-\beta), \quad I(L_0) \sim c(3-\beta)^{5/2}$$

and

$$\frac{\theta_1}{\theta_2} \sim c(3-\beta)$$

as $\beta \to 3$. Therefore in (5.11) we have

$$\text{l.h.s.} \sim c(3-\beta)^2 \text{ and r.h.s. } \sim c(3-\beta)^{5/2}$$

and so (5.11) does not hold if β is sufficiently close to 3. For increasing β at some threshold β_0 with $0 < \beta < 3$ both spike locations L approach the same positive limit which is given by L_0 evaluated at β_0. For $\beta_0 < \beta < 3$ the spikes near the jump cease to exist.

(ii) If $x_b \to 1$, we get $\tanh \theta_2(1-x_b) \to 0$. This implies that we also have $\beta \to 3$. Repeating the previous analysis, we get

$$e^{-2L_0} \sim c(3-\beta), \quad I(L_0) \sim c(3-\beta)^{5/2}$$

and

$$\frac{\theta_1}{\theta_2} \sim c$$

as $\beta \to 3$. Arguing similarly as in Case (i), we see that spikes near the jump cease to exist. In Corollary 3.6 and Remark 3.7 this argument has been made quantitative and explicit bounds for nonexistence have been derived.

(iii) If $\beta \to 0$, from (5.7) we get

$$(\theta_2^2 - \theta_1^2) \int_L^\infty w^3(y)\rho(y)\, dy \to 0.$$

For $\theta_2^2 - \theta_1^2 \neq 0$, this implies that $L \to -\infty$ or $L \to \infty$. In this limit, the spikes at the jump connect to the interior spikes, which converge to the jump.

(iv) The case when $\beta \to 0$ and simultaneously $\theta_2 \to \theta_1 := \theta$ requires further investigation. An example for this coincidence is given by $x_b = 0$. Then (5.7) implies

$$5.4\,[1 + \theta(\tanh\theta - \coth\theta)] = \int_L^\infty w^3(y)\rho(y)\, dy.$$

This equation has a solution iff

$$5.4\,[1 + \theta(\tanh\theta - \coth\theta)] < \int_0^\infty w^3(y)\rho(y)\, dy = 4.640625. \tag{5.12}$$

It is an elementary computation to show that l.h.s. in (5.12) has the limit zero as $\theta \to 0$, is strictly monotone increasing in θ and has the limit 5.4 as $\theta \to \infty$. This implies that (5.7) has a solution iff θ is small enough. Then (5.7) has two solutions L_1 and L_2 with $L_1 = -L_2$. These solutions are symmetric with respect to the jump discontinuity.

6. Numerical computations

We now show some numerical computations for the time-dependent behavior of system (1.1). We choose $\Omega = (-1, 1)$, $\tau = 0.1$ and varying diffusion coefficients ϵ^2. We divide Ω at either $x_b = 0$ or $x_b = 0.5$ and choose different constants for $D(x)$ on each of the resulting subintervals.

In each situation we present the solution for $t = 10^5$. By this time the computation has come to a standstill in all cases, and this steady state is numerically stable (long-time limit). For the 1D computations, the first component, a, is shown on the left and the second component, h, is displayed on the right.

We first plot the initial conditions which are the same for all computations. We study the following two examples:

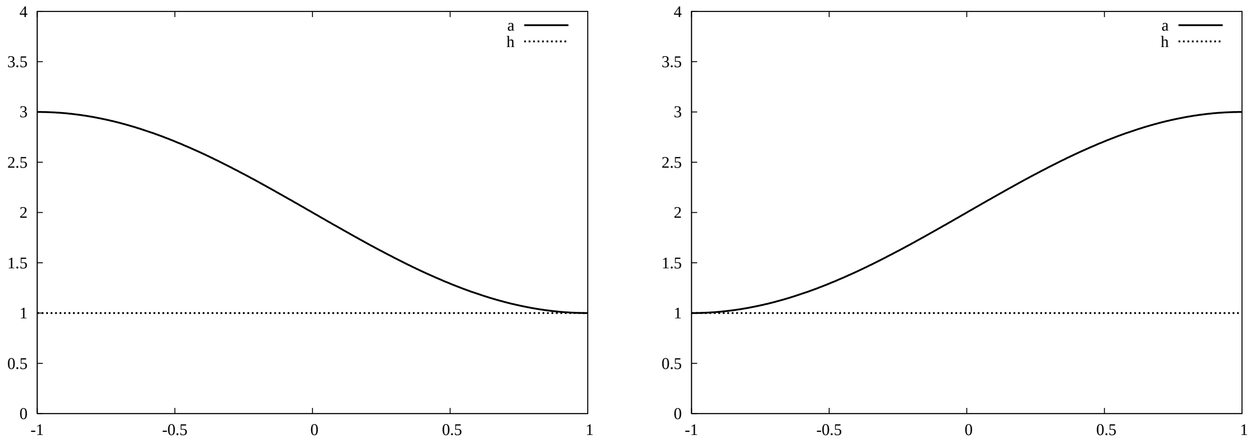

Figure 1. *Initial condition for a at $t = 0$: in the first example we take $a = 2 - \sin(x\pi/2)$, i.e. the maximum is located at the left boundary. In the second example we take $a = 2 + \sin(x\pi/2)$, i.e. the maximum is located at the right boundary. Initial condition for h at $t = 0$: $h = 1$ for both examples. Both examples of initial conditions are investigated for all 1D computations which follow.*

We now show a computation of a spike which either reaches a position near the jump discontinuity of the inhibitor diffusion (moving in from the left) or an interior position (moving in from the right) at $t = 10^5$. The spike near the jump discontinuity is located slightly left of it which corresponds to the stable spike location having $L > 0$.

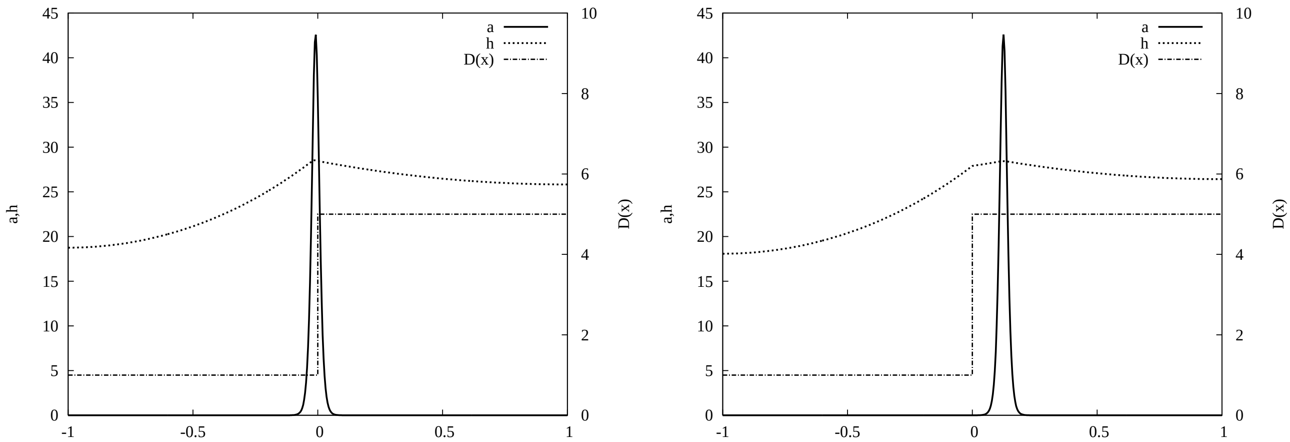

Figure 2. *Long-time limit of the solution to (1.1) – (1.3) with* $\epsilon^2 = 0.0001$ *and* $D(x) = 1$ *for* $-1 < x < 0$, $D(x) = 5$ *for* $0 < x < 1$. *The initial conditions are given in Figure 1. We observe a spike near the jump discontinuity of the inhibitor diffusivity and a spike in the right subinterval. The conditions (3.1) and (3.4), respectively, are satisfied. Equation (3.3) implies* $t_0 \approx 0.10336$ *for the position of the interior spike in the second example, which is in good agreement with the figure.*

Doing the computation with the same two initial conditions but changing the jump discontinuity of the diffusion coefficient of the inhibitor from $x_b = 0$ to $x_b = 0.5$ the result is similar. However, the limit position changes. In both examples the spike moves to the same interior spike which is located near the center $x = 0$.

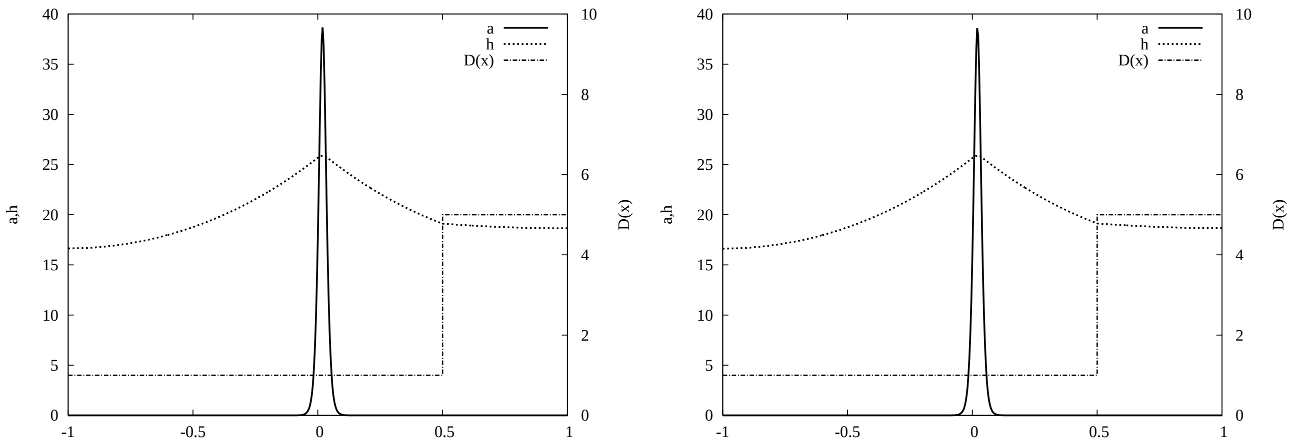

Figure 3. *Long-time limit of the solution to (1.1) – (1.3) with* $\epsilon^2 = 0.0001$ *and* $D(x) = 1$ *for* $-1 < x < 0.5$, $D(x) = 5$ *for* $0.5 < x < 1$. *The initial conditions are given in Figure 1. We observe an interior spike in the left subinterval. The condition (3.1) is satisfied. Equation (3.3) implies* $t_0 \approx 0.01556$ *for the position of the interior spike, which is in good agreement with the figure.*

Now we show the computations for some effects not analyzed in this paper. The initial conditions are again the two examples shown in Figure 1. We compute the following situation: $\epsilon^2 = 0.0001$, $D(x) = 0.1$ for $-1 < x < x_b$, $D(x) = 0.5$ for $x_b < x < 1$ for varying x_b. If we decrease $D(x)$ we expect solutions with multiple spikes. Some examples of this are shown in the following two figures.

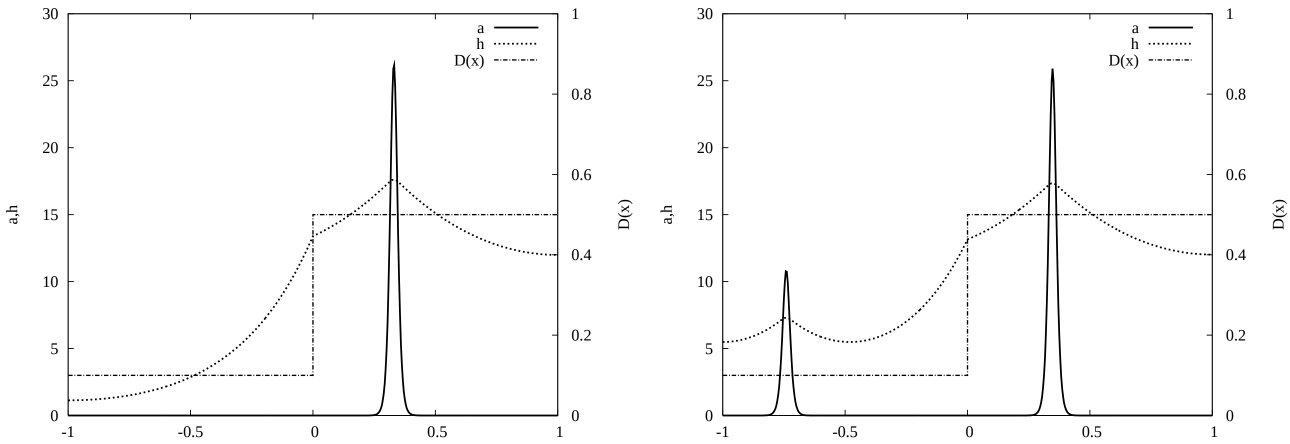

Figure 4. *Long-time limit of the solution to (1.1) – (1.3) with* $\epsilon^2 = 0.0001$ *and* $D(x) = 0.1$ *for* $-1 < x < 0$, $D(x) = 0.5$ *for* $0 < x < 1$. *The initial conditions are given in Figure 1. We observe an interior spike in the right subinterval or two interior spikes in different subintervals. Equation (3.3) implies* $t_0 \approx 0.33057$ *for the position of the interior spike in the first example, which is in good agreement with the figure.*

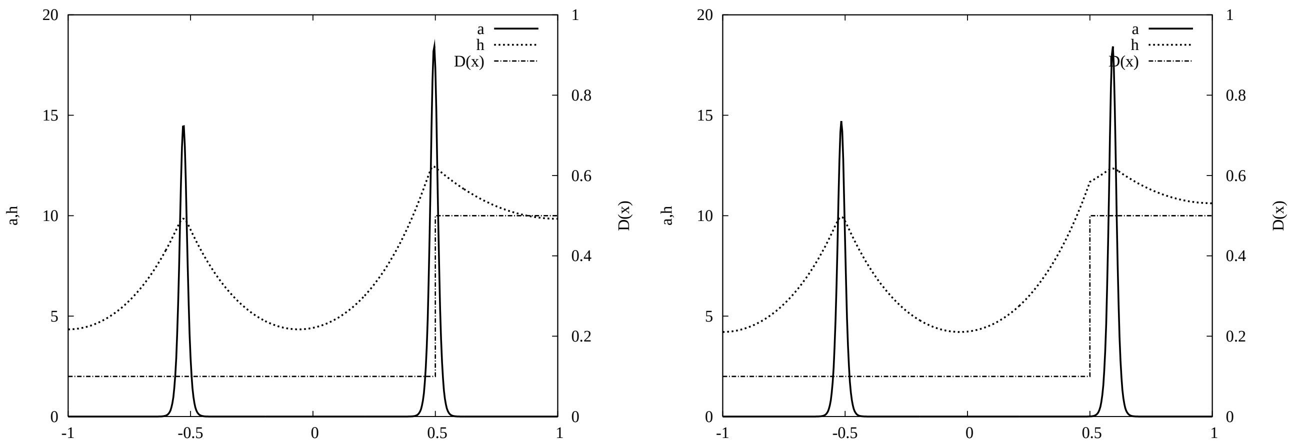

Figure 5. *Long-time limit of the solution to (1.1) – (1.3) with* $\epsilon^2 = 0.0001$ *and* $D(x) = 0.1$ *for* $-1 < x < 0.5$, $D(x) = 0.5$ *for* $0.5 < x < 1$. *The initial conditions are given in Figure 1. We observe an interior spike in the left subinterval combined with a spike near the jump discontinuity or two interior spikes in different subintervals.*

We conclude the computations by showing the results of some two-dimensional computations. The domain is a disc and the diffusion coefficient of the inhibitor jumps along a circle: it is smaller on a small inner disc and larger on an outer annulus. We observe multiple spikes which are denser and have smaller amplitude in the region with smaller diffusion coefficient.

In this figure, we display only the activator, a. We give a 2D and a 3D representation of the solution at $t = 10^5$.

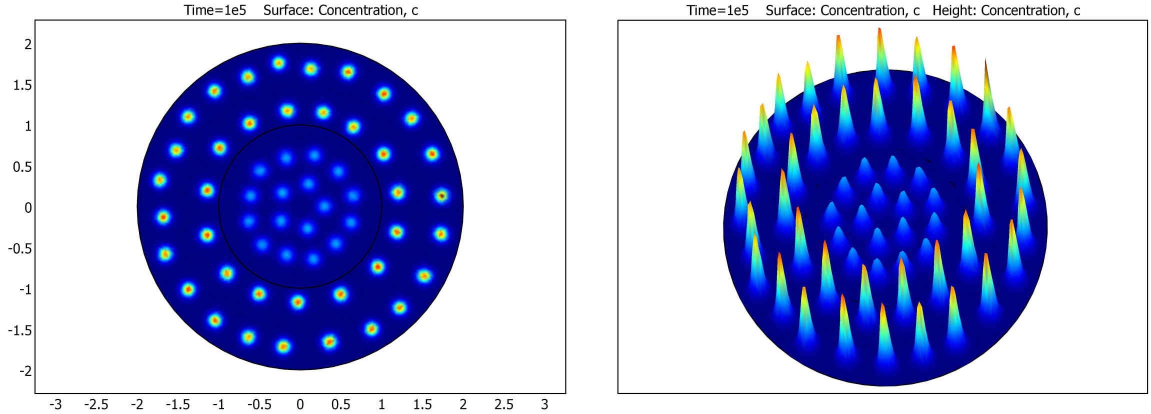

Figure 6. *Long-time limit of the solution to (1.1) – (1.3) in the disc* $|x| < 2$, *where* $\epsilon^2 = 0.001$ *and* $D(x) = 0.01$ *for* $|x| < 1$, $D(x) = 0.05$ *for* $1 < |x| < 2$. *The maximum value for a is about 10.158. In the inner disc of the domain, where the diffusion coefficient is smaller than in the outer annulus, we observe multiple spikes which are denser and have smaller amplitude.*

7. Discussion

It is seen in the numerical computations given in the previous section that dynamically, if a spike moves away from the left or right boundary, driven by the gradient of the regular part of the Green's function, it converges to the closest stationary stable spike, either an interior spike or a spike near the jump discontinuity. This includes the possibility that the spike crosses the jump discontinuity and moves from one subinterval into the other if there is no stable spike at the jump discontinuity.

The numerical computations support the conjecture that one of spikes near the jump discontinuity given in Theorem 3.4 is stable while the other one is unstable. The dynamical system seems to select this stable position in the long-time limit. The spike does not stop at the unstable position.

This dynamical behavior is simpler than in [15]. In that work traveling pulses for heterogeneous systems close to bifurcation points such as drift instability or splitting instability are considered. Many different types of dynamical behavior occur such as pinning, splitting, rebound, penetration or oscillation. The system studied in the current paper is far from any bifurcation point and the movement of the spike is driven by the gradient of the regular part of the Green's function. Therefore the direction and the speed of the spike at each point are uniquely defined. Penetration or pinning are possible but we do not get splitting, rebound or oscillation.

Steady states with two spikes (which are possible for smaller diffusion constants) display several interesting phenomena. Numerical computations show that there are many possible combinations such as two interior spikes in the same subinterval, two interior spikes in different subintervals or a spike near the jump discontinuity and an interior spike. In these solutions the two spikes in general have different amplitudes unless they are both located in the same subinterval.

Boundaries are frequently formed as a result of varying genetic expressions. The following situations are well understood [4], [5], [10]. The A-P and D-V boundaries in the *Drosophila* wing imaginal disc and the compartments in the vertebrate hindbrain are examples of lineage boundaries: they are established because of varying gene expressions in different compartments, and due to varying adhesion effects only a small percentage of cells cross the boundary to move into the neighboring compartment. The imaginal disc consists of a group of cells which form adult structures during metamorphosis. Investigating the mechanisms of their interaction is crucial in understanding how a larva develops into a fly. After establishment of the compartments often special border cells are created. They play an important role for morphogenesis by acting as a signaling center which determines the further progress of patterning.

A model which explains the role of boundaries as organizing regions for secondary embryonic fields has been introduced by Meinhardt [12] following the concept of positional information due to Wolpert [26]. Within this framework it is postulated that near a sharp border a spike for the morphogen concentration appears. We support this postulate by showing that in a simple activator-inhibitor system it is possible to have a stable spike for one of the morphogens near a jump of the inhibitor diffusivity which models this sharp border. Using this postulate, various biological examples have been explained such as the formation of duplicated and triplicated insect legs and the regeneration-duplication phenomenon of imaginal disc fragments.

A phenomenon similar to the one discussed in this paper is the well known distinction between so-called body modes (states localized away from boundaries) and wall modes (states localized near boundaries) which play a role in various branches of physics such as fluid mechanics [13] or plasma physics [6].

To conclude, the effects explored in this paper such as asymmetric positions or amplitudes of spikes as well as localization of patterns to a sub-domain play an important role in biological modeling, for example in the development of skeletal patterns in growing vertebrate limbs or for compartment boundaries of differently determined cell types. We plan to shed further light on these issues in the future, combining analysis with computation and applying the outcomes to various biological models.

8. Appendix A: introduction and analysis of the Green's function

Let $G(x,t_0)$ be the Green's function which is defined as the unique solution of the problem

$$\begin{cases} (D(x)G(x,t_0)_x)_x - G(x,t_0) + \delta_{t_0} = 0, \quad G_x(-1,t_0) = G_x(1,t_0) = 0, \\ D(t_0)G_x(t_0^-,t_0) - D(t_0)G_x(t_0^+,t_0) = 1, \qquad G(t_0^-,t_0) - G(t_0^+,t_0) = 0, \\ D(x_b^-)G_x(x_b^-,t_0) - D(x_b^+)G_x(x_b^+,t_0) = 0, \quad G(x_b^-,t_0) - G(x_b^+,t_0) = 0, \end{cases} \tag{8.1}$$

where δ_{t_0} is the Dirac delta distribution located at t_0.

Setting

$$G(x,t_0) = \begin{cases} A\dfrac{\cosh\theta_1(x+1)}{\cosh\theta_1(t_0+1)}, & -1 < x < t_0, \\[2ex] B\dfrac{\sinh\theta_1(x-t_0)}{\sinh\theta_1(x_b-t_0)} + A\dfrac{\sinh\theta_1(x-x_b)}{\sinh\theta_1(t_0-x_b)}, & t_0 < x < x_b, \\[2ex] B\dfrac{\cosh\theta_2(x-1)}{\cosh\theta_2(x_b-1)}, & x_b < x < 1 \end{cases} \tag{8.2}$$

then $G(x,t_0)$ is continuous at both $x = t_0$ and $x = x_b$. Using the conditions that $D(x)G_x(x,t_0)$ jumps by -1 at $x = t_0$ and is continuous at $x = x_b$, we get

$$\begin{aligned} \frac{A}{\theta_1}\left(\tanh\theta_1(t_0+1) + \coth\theta_1(x_b-t_0)\right) - \frac{B}{\theta_1}\frac{1}{\sinh\theta_1(x_b-t_0)} &= 1, \\ B\left(\frac{1}{\theta_1}\coth\theta_1(x_b-t_0) + \frac{1}{\theta_2}\tanh\theta_2(1-x_b)\right) - \frac{A}{\theta_1}\frac{1}{\sinh\theta_1(x_b-t_0)} &= 0. \end{aligned} \tag{8.3}$$

From (8.3) we compute

$$G(t_0,t_0)^{-1} = A^{-1} = \theta_1^{-1}\Bigg[\tanh\theta_1(t_0+1) + \coth\theta_1(x_b-t_0) \tag{8.4}$$

$$-\left(\sinh\theta_1(x_b-t_0)\cosh\theta_1(x_b-t_0) + \frac{\theta_1}{\theta_2}\sinh^2\theta_1(x_b-t_0)\tanh\theta_2(1-x_b)\right)^{-1}\Bigg]$$

$$= \theta_1^{-1}\left[\tanh\theta_1(t_0+1) + \frac{\theta_2\sinh\theta_1(x_b-t_0) + \theta_1\cosh\theta_1(x_b-t_0)\tanh\theta_2(1-x_b)}{\theta_2\cosh\theta_1(x_b-t_0) + \theta_1\sinh\theta_1(x_b-t_0)\tanh\theta_2(1-x_b)}\right] =: \theta_1^{-1}u(t_0).$$

Setting $v(t_0) = \theta_2\cosh\theta_1(x_b-t_0) + \theta_1\sinh\theta_1(x_b-t_0)\tanh\theta_2(1-x_b)$, we have

$$u(t_0) \quad = \quad \tanh\theta_1(t_0+1) - \theta_1^{-1}\frac{v'(t_0)}{v(t_0)}.$$

Note that $\theta_1^{-2}v''(t_0) = v(t_0)$. This implies for $u'(t_0) = \frac{d}{dt_0}u(t_0)$ that

$$\begin{aligned}\theta_1^{-1}u'(t_0) &= 1 - \tanh^2\theta_1(t_0+1) - \theta_1^{-2}\frac{v''(t_0)v(t_0) - (v'(t_0))^2}{(v(t_0))^2} \\ &= -\tanh^2\theta_1(t_0+1) + \theta_1^{-2}\frac{(v'(t_0))^2}{(v(t_0))^2}. \end{aligned} \tag{8.5}$$

Note that $\frac{d}{dt_0}G(t_0,t_0) = 0$ iff $u'(t_0) = 0$ and $u(t_0) \neq 0$, since

$$\frac{d}{dt_0}G(t_0,t_0) = -\theta_1\frac{u'(t_0)}{(u(t_0))^2}. \tag{8.6}$$

Next we compute

$$\begin{aligned}\theta_1^{-2}u''(t_0) &= -2\tanh\theta_1(t_0+1)(1-\tanh^2\theta_1(t_0+1)) \\ &\quad +2\theta_1^{-3}\frac{v(t_0)v'(t_0)v''(t_0) - v(t_0)(v'(t_0))^3}{(v(t_0))^3} \\ &= -2\tanh\theta_1(t_0+1)(1-\tanh^2\theta_1(t_0+1)) \\ &\quad +2\theta_1^{-3}\frac{v'(t_0)[\theta_1^2(v(t_0))^2 - (v'(t_0))^2]}{(v(t_0))^3}.\end{aligned}$$

Using the relations

$$\theta_1^2(v(t_0))^2 - (v'(t_0))^2 = \theta_1^2\theta_2^2\left[1 - \left(\frac{\theta_1}{\theta_2}\tanh\theta_2(1-x_b)\right)^2\right] > 0$$

(by (3.1)) and $v'(t_0) < 0$, we get $u''(t_0) < 0$. To determine the sign of $\frac{d^2}{dt_0^2}G(t_0,t_0)$, we compute

$$\frac{d^2}{dt_0^2}G(t_0,t_0) \quad = \quad \theta_1\frac{-u''(t_0)u(t_0) + 2(u'(t_0))^2}{(u(t_0))^3}.$$

Noting that $u'(t_0) = 0$ and $u''(t_0) < 0$, we get

$$\frac{d^2}{dt_0^2}G(t_0,t_0) > 0. \tag{8.7}$$

This will imply that the interior spike is linearly stable. The proof of this statement will be given in Appendix E.

Now we study further properties of the Green's function G. For $t_0 \in (-1,1)$ we consider $G(t_0,t_0)$. We define the regular part of the Green's function as

$$H(x,y) := \frac{\theta_i}{2} e^{-\theta_i|x-y|} - G(x,y).$$

Then we compute

$$\frac{d}{dt_0}G(t_0,t_0) = \frac{d}{dt_0}\frac{\theta_i}{2} - \frac{d}{dt_0}H(t_0,t_0) = -\,2\nabla_x|_{x=t_0} H(x,t_0) =: -2\nabla_{t_0}H(t_0,t_0), \tag{8.8}$$

where $i=1$ if $t_0 < x_b$ and $i=2$ if $t_0 > x_b$. Here we have used the symmetry of $H(x,y)$ and the notation

$$\nabla_x|_{x=t_0}H(x,t_0) := \frac{\partial}{\partial x}|_{x=t_0}H(x,t_0).$$

Further, we compute

$$\frac{d^2}{dt_0^2}G(t_0,t_0) = -2(\nabla_x\nabla_y)_{x=y=t_0}H(x,y) - 2(\nabla_x^2)_{x=t_0}H(x,t_0) =: -2\nabla_{t_0}^2 H(t_0,t_0). \tag{8.9}$$

Note that $\hat{\xi}(t)$, which has been defined in (4.6), is in $C^1(-1,1)$. We now compute $\nabla_t\hat{\xi}(t)$:

$$\nabla_t\hat{\xi}(t) \;=\; \frac{d}{dt}(G(t,t))^{-1} = 2\nabla_t(G(t,t))^{-1} = -2(\nabla_t G(t,t))\hat{\xi}(t)^2.$$

We also need to know the derivative of the function

$$F(t) := \left(-2\nabla_t G(t,t)\right)\hat{\xi}^2(t) = \nabla_t\hat{\xi}(t).$$

We compute

$$\nabla_t F(t) = \nabla_t \frac{-2\nabla_t G(t,t)}{G^2(t,t)} = \frac{-2G(t,t)\nabla_t^2 G(t,t) + 4\left(\nabla_t G(t,t)\right)^2}{G^3(t,t)},$$

which implies that

$$\nabla_{t_0}F(t_0) = \frac{-2G(t_0,t_0)\nabla_{t_0}^2 G(t_0,t_0)}{G^3(t_0,t_0)} \tag{8.10}$$

if $\nabla_{t_0}G(t_0,t_0) = 0$ which will be assumed in (11.7) below.

9. Appendix B: estimates for the approximate steady state

For $A = w_{\epsilon,t}$, where $w_{\epsilon,t}$ is defined in (4.9), let us compute

$$\tau := T[A](t_0). \tag{9.1}$$

From (4.10), we have

$$
\begin{aligned}
\tau &= T[A](t_0) = \int_{-1}^{1} G(t_0, z) A^2(z)\, dz \\
&= \xi_0^2 \int_{-1}^{1} G(t_0, z) \tilde{w}_0^2(z)\, dz \\
&= \xi_0^2 \epsilon \left[G(t_0, t_0) \int_{-\infty}^{+\infty} w^2(y)\, dy + O(\epsilon) \right] \\
&= \xi_\epsilon \left[G(t_0, t_0) \hat{\xi}_0^2 + O(\epsilon) \right] \qquad \text{(by (4.8))} \\
&= \xi_\epsilon [\hat{\xi}_0 + O(\epsilon)] \qquad \text{(by (4.6)).}
\end{aligned} \tag{9.2}
$$

Let $x = t_0 + \epsilon y$, $z = t_0 + \epsilon \tilde{z}$, where $x, z \in B_{\epsilon^{3/4}}(t_0)$. We calculate

$$
\begin{aligned}
& T[A](x) - T[A](t_0) = \\
&= \int_{-1}^{1} [G(x, z) - G(t_0, z)] A^2(z)\, dz \\
&= \xi_0^2 \int_{-1}^{1} [G(x, z) - G(t_0, z)] \tilde{w}_0^2(z)\, dz \\
&= \xi_0^2 \int_{-1}^{1} [K(|x - z|) - K(|t_0 - z|)] \tilde{w}_0^2(z)\, dz - \xi_0^2 \int_{-1}^{1} [H(x, z) - H(t_0, z)] \tilde{w}_0^2(z)\, dz \\
&= \epsilon^2 \xi_0^2 \left[\int_{-\infty}^{+\infty} \left[\frac{\theta_i^2}{2} |\tilde{z}| - \frac{\theta_i^2}{2} |y - \tilde{z}| \right] w^2(\tilde{z})\, d\tilde{z} + O(\epsilon y^2 + \epsilon^2) \right] \\
&\quad + \epsilon^2 \xi_0^2 \left[-\nabla_x H(x, t_0)|_{x=t_0}\, y \int_{-\infty}^{+\infty} w^2(z)\, dz + O(\epsilon y^2 + \epsilon^2) \right] \\
&= \epsilon^2 \xi_0^2 P_0(y) + \epsilon^2 \xi_0^2 \int_{-\infty}^{+\infty} w^2(z)\, dz\ [-\nabla_x H(x, t_0)|_{x=t_0}]\ y + O(\epsilon y^2 + \epsilon^2) \\
&= \epsilon \xi_\epsilon \left\{ \hat{\xi}_0^2 \frac{P_0(y)}{\int_{-\infty}^{\infty} w^2(z)\, dz} + \hat{\xi}_0^2 [-\nabla_x H(x, t_0)|_{x=t_0}]\, y + O(\epsilon y^2 + \epsilon^2) \right\}
\end{aligned} \tag{9.3}
$$

by (4.8), where

$$
P_0(y) = \int_{-\infty}^{+\infty} \left[\frac{\theta_i^2}{2} |z| - \frac{\theta_i^2}{2} |y - z| \right] w^2(z)\, dz \tag{9.4}
$$

Note that the function $P_0(y)$ is even in y.

For a function $A \in L^2(-1, 1)$, let

$$
S_\epsilon[A] = \epsilon^2 \Delta A - A + \frac{A^2}{T[A]}, \tag{9.5}
$$

where $T[A]$ is given by (4.10). We now set $A = w_{\epsilon,t}$ and compute $S_\epsilon[w_{\epsilon,t}]$.

In fact,

$$
\begin{aligned}
S_\epsilon[w_{\epsilon,t}] &= \epsilon^2 \Delta w_{\epsilon,t} - w_{\epsilon,t} + \frac{w_{\epsilon,t}^2}{T[w_{\epsilon,t}]} \\
&= \xi_0(\epsilon^2\Delta \tilde{w}_0 - \tilde{w}_0) + \frac{w_{\epsilon,t}^2}{T[w_{\epsilon,t}]} + \text{e.s.t.} \\
&= \frac{\xi_0^2 \tilde{w}_0^2}{T[w_{\epsilon,t}]} - \xi_0 \tilde{w}_0^2 + \text{e.s.t.} \\
&= E_1 + \text{e.s.t.}, \qquad (9.6)
\end{aligned}
$$

where

$$
E_1 = \frac{\xi_0^2 \tilde{w}_0^2}{T[w_{\epsilon,t}]} - \xi_0 \tilde{w}_0^2. \qquad (9.7)
$$

Now we estimate E_1, using (9.2), (9.3):

$$
\begin{aligned}
\xi_\epsilon^{-1} E_1 &= \frac{\xi_0^2 \tilde{w}_0^2}{T[w_{\epsilon,t}]}\xi_\epsilon^{-1} - \hat{\xi}_0 \tilde{w}_0^2 \qquad (9.8) \\
&= \frac{(\xi_0\tilde{w}_0)^2}{T[w_{\epsilon,t}](t_0)}\xi_\epsilon^{-1} - \hat{\xi}_0\tilde{w}_0^2 - \frac{(\xi_0\tilde{w}_0)^2}{(T[w_{\epsilon,t}](t_0))^2}(T[w_{\epsilon,t}] - T[w_{\epsilon,t}](t_0))\xi_\epsilon^{-1} \\
&\quad + O\left(|T[w_{\epsilon,t}] - T[w_{\epsilon,t}](t_0)|^2 \epsilon \tilde{w}_0^2\right) \\
&= \tilde{w}_0^2\left(\frac{\hat{\xi}_0^2}{\hat{\xi}_0} - \hat{\xi}_0\right) - \hat{\xi}_0\tilde{w}_0^2 \frac{T[w_{\epsilon,t}] - T[w_{\epsilon,t}](t_0)}{T[w_{\epsilon,t}](t_0)} + O\left(\epsilon^2 y^2 \tilde{w}_0^2\right) \\
&= -\epsilon \tilde{w}_0^2 \left\{ \hat{\xi}_0^2 \frac{P_0(y)}{\int_{-\infty}^{\infty} w^2(z)\,dz} + \hat{\xi}_0^2[-\nabla_x H(x,t_0)|_{x=t_0}]\, y \right\} + O\left(\epsilon^2 y^2 \tilde{w}_0^2\right).
\end{aligned}
$$

This implies that

$$
\xi_\epsilon^{-1}\|E_1\|_{L^2(R)} = O(\epsilon). \qquad (9.9)
$$

From (9.6), we conclude that

$$
\xi_\epsilon^{-1}\|S_\epsilon[w_{\epsilon,t}]\|_{L^2(R)} = O(\epsilon). \qquad (9.10)
$$

10. Appendix C: the Liapunov-Schmidt reduction

In this appendix we study the linear operator defined by

$$
\tilde{L}_{\epsilon,t}\phi := S_\epsilon'[A]\phi = \epsilon^2\Delta\phi - \phi + \frac{2A\phi}{T[A]} - \frac{A^2}{(T[A])^2}(T'[A]\phi), \quad H_N^2(\Omega) \to L^2(\Omega),
$$

where $A = w_{\epsilon,t}$ and for $\phi \in L^2(\Omega)$ the function $T'[A]\phi$ is defined as the unique solution in $H_N^{2,*}(\Omega)$ of

$$
(D(x)(T'[A]\phi)_x)_x - (T'[A]\phi) + 2A\phi = 0, \quad -1 < x < 1. \qquad (10.1)
$$

We define the approximate kernel and co-kernel of the operator $\tilde{L}_{\epsilon,t}$ as follows:

$$\mathcal{K}_{\epsilon,t} := \text{span}\left\{\frac{d\tilde{w}_0}{dx}\right\} \subset H^2_N(\Omega),$$

$$\mathcal{C}_{\epsilon,t} := \text{span}\left\{\frac{d\tilde{w}_0}{dx}\right\} \subset L^2(\Omega).$$

We also introduce the orthogonal projection $\pi^\perp_{\epsilon,t} : L^2(\Omega) \to \mathcal{C}^\perp_{\epsilon,t}$ and study the operator $L_{\epsilon,t} := \pi^\perp_{\epsilon,t} \circ \tilde{L}_{\epsilon,t}$. By letting $\epsilon \to 0$, we will show that $L_{\epsilon,t} : \mathcal{K}^\perp_{\epsilon,t} \to \mathcal{C}^\perp_{\epsilon,t}$ is invertible with a uniformly bounded inverse provided ϵ is sufficiently small. This statement is contained in the following proposition.

Proposition 10.1. *There exist positive constants $\bar{\epsilon}$, λ such that for all $\epsilon \in (0, \bar{\epsilon})$ and all $t \in B_{\epsilon^{3/4}}(t_0)$ we have*

$$\|L_{\epsilon,t}\phi_\epsilon\|_{L^2(\Omega_\epsilon)} \geq \lambda \|\phi_\epsilon\|_{H^2(\Omega_\epsilon)}. \tag{10.2}$$

Further, the map

$$L_{\epsilon,t} = \pi^\perp_{\epsilon,t} \circ \tilde{L}_{\epsilon,t} : \mathcal{K}^\perp_{\epsilon,t} \to \mathcal{C}^\perp_{\epsilon,t}$$

is surjective.

Proof: The proof is given in Proposition 5.1 of [25].

□

Now we are in a position to solve the equation

$$\pi^\perp_{\epsilon,t} \circ S_\epsilon(w_{\epsilon,t} + \phi) = 0, \quad \phi \in \mathcal{K}^\perp_{\epsilon,t}. \tag{10.3}$$

Since by Proposition 10.1 $L_{\epsilon,t} : \mathcal{K}^\perp_{\epsilon,t} \to \mathcal{C}^\perp_{\epsilon,t}$ is invertible (call the inverse $L^{-1}_{\epsilon,t}$), this is equivalent to

$$\phi = -(L^{-1}_{\epsilon,t} \circ \pi^\perp_{\epsilon,t})(S_\epsilon[w_{\epsilon,t}]) - (L^{-1}_{\epsilon,t} \circ \pi^\perp_{\epsilon,t})(N_{\epsilon,t}[\phi]) =: M_{\epsilon,t}[\phi], \quad \phi \in \mathcal{K}^\perp_{\epsilon,t}, \tag{10.4}$$

where

$$N_{\epsilon,t}[\phi] = S_\epsilon[w_{\epsilon,t} + \phi] - S_\epsilon[w_{\epsilon,t}] - S'_\epsilon[w_{\epsilon,t}]\phi.$$

We are going to show that the operator $M_{\epsilon,t}$ defined by (10.4) is a contraction mapping on

$$B_{\epsilon,\delta} := \{\phi \in \mathcal{K}^\perp_{\epsilon,t} : \|\phi\|_{H^2(\Omega_\epsilon)} < \delta\}$$

if δ and ϵ are sufficiently small. We have by (9.9) and Proposition 10.1

$$\begin{aligned}\xi_\epsilon^{-1}\|M_{\epsilon,t}[\phi]\|_{H^2(\Omega_\epsilon)} &\leq \lambda^{-1}\xi_\epsilon^{-1}\left(\left\|\pi^\perp_{\epsilon,t}(N_{\epsilon,t}[\phi])\right\|_{L^2(\Omega_\epsilon)}+\left\|\pi^\perp_{\epsilon,t}(S_\epsilon[w_{\epsilon,t}])\right\|_{L^2(\Omega_\epsilon)}\right)\\ &\leq \lambda^{-1}C\left(\xi_\epsilon^{-1}\delta^2+\epsilon\,|\nabla_t G(t,t)|\right),\end{aligned}$$

where $\lambda > 0, C > 0$ are independent of $\delta > 0$, $\epsilon > 0$. Similarly, it follows that

$$\xi_\epsilon^{-1}\left\|M_{\epsilon,t}[\phi]-M_{\epsilon,t}[\phi']\right\|_{H^2(\Omega_\epsilon)} \leq \lambda^{-1}C\left(\xi_\epsilon^{-1}\delta^2+\epsilon\,|\nabla_t G(t,t)|\right)\|\phi-\phi'\|_{H^2(\Omega_\epsilon)},$$

where $\lambda > 0$, $C > 0$ are independent of $\delta > 0$, $\epsilon > 0$.

By the previous two estimates, if we choose δ and ϵ sufficiently small, then $M_{\epsilon,t}$ is a contraction mapping on $B_{\epsilon,\delta}$. The existence of a fixed point $\phi_{\epsilon,t}$ now follows from the contraction mapping principle and $\phi_{\epsilon,t}$ is the unique solution of (10.4).

We have thus proved the following result.

Lemma 10.2. *There exists $\bar\epsilon > 0$ such that for every pair of ϵ, t with $0 < \epsilon < \bar\epsilon$ and $t \in B_{\epsilon^{3/4}}(t_0)$ there exists a unique $\phi_{\epsilon,t} \in \mathcal{K}^\perp_{\epsilon,t}$ satisfying $S_\epsilon(w_{\epsilon,t}+\phi_{\epsilon,t}) \in \mathcal{C}_{\epsilon,t}$. Further, we have the estimate*

$$\xi_\epsilon^{-1}\|\phi_{\epsilon,t}\|_{H^2(\Omega_\epsilon)} \leq C\epsilon. \tag{10.5}$$

11. Appendix D: the reduced problem

In this appendix we derive a reduced problem which will be essential for the proof of the existence results.

By Lemma 10.2, for every $t \in B_{\epsilon^{3/4}}(t_0)$ there exists a unique solution $\phi_{\epsilon,t} \in \mathcal{K}^\perp_{\epsilon,t}$ such that

$$S_\epsilon[w_{\epsilon,t}+\phi_{\epsilon,t}] = v_{\epsilon,t} \in \mathcal{C}_{\epsilon,t}. \tag{11.1}$$

Our idea is to find $t^\epsilon \in B_{\epsilon^{3/4}}(t_0)$ such that in addition

$$S_\epsilon[w_{\epsilon,t^\epsilon}+\phi_{\epsilon,t^\epsilon}] \perp \mathcal{C}_{\epsilon,t^\epsilon}. \tag{11.2}$$

Then from (11.1) and (11.2) we get that $S_\epsilon[w_{\epsilon,t^\epsilon}+\phi_{\epsilon,t^\epsilon}] = 0$. To this end, we let

$$W_\epsilon(t) \;:=\; \xi_\epsilon^{-1}\epsilon^{-1}\int_\Omega S[w_{\epsilon,t}+\phi_{\epsilon,t}]\frac{d\tilde w_0}{dx}\,dx, \quad B_{\epsilon^{3/4}}(t_0)\to R.$$

Then the problem is reduced to finding a zero of the function $W_\epsilon(t)$ in $B_{\epsilon^{3/4}}(t_0)$.

Let us now calculate $W_\epsilon(t)$. We have

$$\begin{aligned}\xi_\epsilon^{-1}\epsilon^{-1}\int_\Omega S[w_{\epsilon,t}+\phi_{\epsilon,t}]\frac{d\tilde{w}_0}{dx}\,dx &= \xi_\epsilon^{-1}\epsilon^{-1}\int_\Omega S[w_{\epsilon,t}]\frac{d\tilde{w}_0}{dx}\,dx\\ &\quad+\xi_\epsilon^{-1}\epsilon^{-1}\int_\Omega S'_\epsilon[w_{\epsilon,t}]\phi_{\epsilon,t}\frac{d\tilde{w}_0}{dx}\,dx+\xi_\epsilon^{-1}\epsilon^{-1}\int_\Omega N_{\epsilon,t}[\phi_{\epsilon,t}]\frac{d\tilde{w}_0}{dx}\,dx\\ &= I_1+I_2+I_3,\end{aligned}$$

where I_1, I_2 and I_3 are defined by the last equality.

The computation of I_3 is the easiest: note that the first term in the expansion of $N_{\epsilon,t}$ is quadratic in $\phi_{\epsilon,t}$ and so

$$I_3 = O(\epsilon^2). \tag{11.3}$$

Now we compute I_1 and I_2. The result will be that I_1 is the leading term and $I_2 = O(\epsilon)$.

For I_1, we have

$$I_1 = \xi_\epsilon^{-1}\epsilon^{-1}\int_\Omega E_1\frac{d\tilde{w}_0}{dx}\,dx + O(\epsilon), \tag{11.4}$$

where E_1 has been defined in (9.7).

We calculate, using (9.8) and the fact that $P_0(y)$ is an even function

$$\begin{aligned}I_1 &= \xi_\epsilon^{-1}\epsilon^{-1}\int_\Omega E_1\frac{d\tilde{w}_0}{dx}\,dx\\ &= -\int_R \tilde{w}_0^2\left[\hat{\xi}_0^2[-\nabla_x H(x,t_0)|_{x=t_0}]y\right]\tilde{w}_0'\,dy + O(\epsilon)\\ &= \hat{\xi}_0^2\int_R \left(yw^2w'\right)dy[\nabla_x H(x,t_0)|_{x=t_0}] + O(\epsilon)\\ &= -\frac{1}{3}\hat{\xi}_0^2\int_R w^3 dy[\nabla_x H(x,t_0)|_{x=t_0}] + O(\epsilon).\end{aligned}$$

Then, by using (2.3), we have

$$I_1 = -d_{00}[\nabla_x H(x,t_0)|_{x=t_0}] + O(\epsilon), \tag{11.5}$$

where

$$d_{00} = 2.4\hat{\xi}_0^2.$$

For I_2, we calculate

$$\begin{aligned}
I_2 &= \xi_\epsilon^{-1}\epsilon^{-1}\int_\Omega S_\epsilon'[w_{\epsilon,t}](\phi_{\epsilon,t})\frac{d\tilde{w}_0}{dx}\,dx \\
&= \xi_\epsilon^{-1}\epsilon^{-1}\int_\Omega \left[\epsilon^2\Delta\phi_{\epsilon,t}-\phi_{\epsilon,t}+\frac{2w_{\epsilon,t}\phi_{\epsilon,t}}{T[w_{\epsilon,t}]}-\frac{w_{\epsilon,t}^2}{(T[w_{\epsilon,t}])^2}(T'[w_{\epsilon,t}]\phi_{\epsilon,t})\right]\frac{d\tilde{w}_0}{dx}\,dx \\
&= \xi_\epsilon^{-1}\epsilon^{-1}\int_\Omega \left[\epsilon^2\Delta\frac{d\tilde{w}_0}{dx}-\frac{d\tilde{w}_0}{dx}+\frac{2w_{\epsilon,t}}{T[w_{\epsilon,t}](t_0)}\right]\phi_{\epsilon,t}\,dx \\
&\quad +\xi_\epsilon^{-1}\epsilon^{-1}\int_\Omega \frac{2w_{\epsilon,t}}{T[w_{\epsilon,t}](t_0)}\phi_{\epsilon,t}\left(\frac{T[w_{\epsilon,t}](t_0)-T[w_{\epsilon,t}]}{T[w_{\epsilon,t}]}\right)dx \\
&\quad -\xi_\epsilon^{-1}\epsilon^{-1}\int_\Omega \frac{w_{\epsilon,t}^2}{(T[w_{\epsilon,t}])^2}(T'[w_{\epsilon,t}]\phi_{\epsilon,t})\frac{d\tilde{w}_0}{dx}\,dx+O(\epsilon^2)=O(\epsilon)
\end{aligned}$$

by (4.5), (9.2), (9.3) since

$$\|\phi_{\epsilon,t}\|_{H^2(\Omega_\epsilon)}=O(\epsilon).$$

Combining I_1, I_2 and I_3, we have

$$W_\epsilon(t)=-d_{00}[\nabla_x H(x,t_0)|_{x=t_0}]+O(\epsilon), \tag{11.6}$$

where

$$d_{00}=2.4\hat{\xi}_0^2.$$

Let us for the moment assume that

$$\nabla_{t_0}H(t_0,t_0)=0 \quad\text{and}\quad \nabla_{t_0}^2 H\,(t_0)\neq 0. \tag{11.7}$$

We will check the conditions in (11.7) at the end of this appendix.

Then the function $W_\epsilon(t)$ satisfies $W_\epsilon(t)=-c\nabla_{t_0}^2 H(t_0,t_0)(t-t_0)+O(\epsilon)$ for some $c>0$.

Thus for ϵ small enough $\nabla_t H(t,t)$ has exactly one zero in $B_{\epsilon^{3/4}}(t_0)$. Further, it has opposite signs for the endpoints of $B_{\epsilon^{3/4}}(t_0)$. Since this property is also true for $W_\epsilon(t)$, by the intermediate value theorem it follows that, for ϵ small enough, there exists a $t^\epsilon\in B_{\epsilon^{3/4}}(t_0)$ such that $W_\epsilon(t^\epsilon)=0$ and $t_\epsilon\to t_0$ as $\epsilon\to 0$.

Thus we have proved the following proposition.

Proposition 11.1. *For ϵ sufficiently small there exists a point $t^\epsilon\in B_{\epsilon^{3/4}}(t_0)$ with $t_\epsilon\to t_0$ such that $W_\epsilon(t^\epsilon)=0$.*

Finally, we prove Theorem 3.1.

Proof of Theorem 3.1: We mention the main steps. By Proposition 11.1, there exists a $t^\epsilon \in B_{\epsilon^{3/4}}(t_0)$ such that $t^\epsilon \to t_0$ and $W_\epsilon(t^\epsilon) = 0$, or, expressed differently, $S_\epsilon[w_{\epsilon,t^\epsilon} + \phi_{\epsilon,t^\epsilon}] = 0$. Let $w_\epsilon = w_{\epsilon,t^\epsilon} + \phi_{\epsilon,t^\epsilon}$. By the Maximum Principle, $w_\epsilon > 0$. Moreover, by its construction, w_ϵ has all the properties required in Theorem 3.1. The proof is finished.

□

It remains to check the conditions in (11.7).

We assume that

$$-1 < t_0 < x_b < 1 \tag{11.8}$$

(This condition holds without loss of generality. The case $-1 < x_b < t_0 < 1$ follows by reflection about $x = 0$ which reverses the signs of of x_b and t_0 and swaps the two diffusion constants θ_1 and θ_2.)

By (8.5), (8.6) together with (8.7), (8.8) and (8.9), we see that $\nabla_{t_0} H(t_0, t_0) = 0$ and $\nabla^2_{t_0} H(t_0, t_0) \neq 0$ if and only if t_0 is a solution of the equation

$$\frac{\sinh \theta_1(t_0+1)}{\cosh \theta_1(t_0+1)} = \frac{\theta_2 \sinh \theta_1(x_b - t_0) + \theta_1 \cosh \theta_1(x_b - t_0) \tanh \theta_2(1 - x_b)}{\theta_2 \cosh \theta_1(x_b - t_0) + \theta_1 \sinh \theta_1(x_b - t_0) \tanh \theta_2(1 - x_b)}.$$

Using elementary algebra, including addition theorems, it is easy to see that this is equivalent to

$$\frac{1}{\theta_1} \tanh \theta_1(2t_0 + 1 - x_b) + \frac{1}{\theta_2} \tanh \theta_2(x_b - 1) = 0,$$

which is equivalent to (3.3). From (11.8), we get

$$-1 - x_b < 2t_0 + 1 - x_b < 1 + x_b.$$

So a necessary condition for solvability of (3.3) is

$$\frac{1}{\theta_1} \tanh\left(\theta_1(1 + x_b)\right) > \frac{1}{\theta_2} \tanh\left(\theta_2(1 - x_b)\right)$$

which is the same as inequality (3.1). Assuming condition (3.1), there exists a unique position t_0 solving (3.3). This follows by elementary considerations, utilizing the continuity and monotonicity of the respective functions.

Now it can be shown rigorously that an interior spike located at t^ϵ with $t^\epsilon \to t_0$ as $\epsilon \to 0$ does exist if ϵ is small enough. The proof uses Liapunov-Schmidt reduction and follows the arguments given in [25]. We omit the technical details.

□

12. Appendix E: the proof of stability of the interior spike

Proof of Theorem 3.3: In this appendix we prove the stability of the interior spike.

We need to analyze the following eigenvalue problem

$$\tilde{L}_{\epsilon,t^\epsilon}\phi_\epsilon = \epsilon^2\Delta\phi_\epsilon - \phi_\epsilon + \frac{2A\phi_\epsilon}{T[A]} - \frac{A^2}{(T[A])^2}(T'[A]\phi_\epsilon) = \lambda_\epsilon\phi_\epsilon, \tag{12.1}$$

where λ_ϵ is some complex number, $A = w_{\epsilon,t^\epsilon} + \phi_{\epsilon,t^\epsilon}$ with $t^\epsilon \in B_{\epsilon^{3/4}}(t_0)$ determined in the previous section and

$$\phi_\epsilon \in H^2_N(\Omega). \tag{12.2}$$

(Recall that $T[A]$ and $T'[A]\phi_\epsilon$ have been defined in (4.10) and (10.1) respectively.)

We first study the eigenvalues with $\lambda_\epsilon \to \lambda_0 \neq 0$ as $\epsilon \to 0$. The key ingredient is Theorem 2.1.

Because we study the large eigenvalues, there exists some small $c > 0$ such that $|\lambda_\epsilon| \geq c > 0$ for ϵ sufficiently small. We are looking for a condition under which Re $(\lambda_\epsilon) < 0$ for all eigenvalues λ_ϵ of (12.1), (12.2) if ϵ is sufficiently small. If $\mathrm{Re}(\lambda_\epsilon) \leq -c$, then λ_ϵ is a stable large eigenvalue. Therefore, for the rest of this section we assume that $\mathrm{Re}(\lambda_\epsilon) \geq -c$ and study the stability properties of such eigenvalues.

In (12.1), (12.2) it is assumed that $\tau = 0$. By a straight-forward perturbation argument all the results also hold true for $0 < \tau < \tau_0$, for some sufficiently small $\tau_0 > 0$ which can be chosen independent of ϵ.

We first rigorously derive the limit problem of (12.1), (12.2) as $\epsilon \to 0$ which will be given by a system of NLEPs. Let us assume that

$$\|\phi_\epsilon\|_{H^2(\Omega_\epsilon)} = 1.$$

We cut off ϕ_ϵ as follows: introduce

$$\phi_{\epsilon,0}(y) = \phi_\epsilon(y)\chi\left(\frac{\epsilon y - t^\epsilon}{r_0}\right), \tag{12.3}$$

where $y = x/\epsilon$ for $x \in \Omega$.

From (12.1), (12.2), using $\mathrm{Re}(\lambda_\epsilon) \geq -c$ and $\|\phi_{\epsilon,t^\epsilon}\|_{H^2(\Omega_\epsilon)} = O(\epsilon)$, it follows that

$$\phi_\epsilon = \phi_{\epsilon,0} + O(\epsilon) \quad \text{in } H^2(\Omega_\epsilon). \tag{12.4}$$

Then, by a standard procedure, we extend $\phi_{\epsilon,0}$ to a function defined on R such that

$$\|\phi_{\epsilon,0}\|_{H^2(R)} \leq C\|\phi_{\epsilon,0}\|_{H^2(\Omega_\epsilon)}.$$

Since $\|\phi_\epsilon\|_{H^2(\Omega_\epsilon)} = 1$, $\|\phi_{\epsilon,0}\|_{H^2(\Omega_\epsilon)} \leq C$. By taking a subsequence of ϵ, we may also assume that $\phi_{\epsilon,0} \to \phi_0$ as $\epsilon \to 0$ in $H^2(R)$.

Sending $\epsilon \to 0$ with $\lambda_\epsilon \to \lambda_0$ and $x \in B_{\epsilon^{3/4}}(t_0)$, (12.1) implies

$$\Delta\phi_0 - \phi_0 + 2w\phi_0 - 2\frac{\int_R w\phi_0\,dy}{\int_R w^2\,dy}w^2 = \lambda_0\phi_0. \tag{12.5}$$

The following result states that the stability for ϵ small enough is the same as the stability for $\epsilon = 0$. Both directions are given by parts (1) and (2) of the theorem respectively. We have

Theorem 12.1. *Let λ_ϵ be an eigenvalue of (12.1) and (12.2) such that $Re(\lambda_\epsilon) > -c$ for some $c > 0$.*

(1) Suppose that (for suitable sequences $\epsilon_n \to 0$) we have $\lambda_{\epsilon_n} \to \lambda_0 \neq 0$. Then λ_0 is an eigenvalue of the problem (NLEP) given in (12.5).

(2) Let $\lambda_0 \neq 0$ with $Re(\lambda_0) > 0$ be an eigenvalue of the problem (NLEP) given in (12.5). Then, for ϵ sufficiently small, there is an eigenvalue λ_ϵ of (12.1) and (12.2) such that $\lambda_\epsilon \to \lambda_0$ as $\epsilon \to 0$.

Proof: (1) of Theorem 12.1 follows by asymptotic analysis similar to Appendix C.

To prove (2) of Theorem 12.1, we use an argument of Dancer given in Section 2 of [7]. For details on how to transfer his argument to the Gierer-Meinhardt system, we refer to [24] where it is applied to a related problem.

□

We now study the stability of (12.1), (12.2).

We can apply Theorem 2.1 (2) with $\gamma = 2$ to (12.5). This implies that

$$\mathrm{Re}(\lambda_0) \leq c_0 < 0 \qquad \text{for some } c_0 > 0.$$

By Theorem 12.1 (1), all eigenvalues λ_ϵ of (12.1), (12.2), for which $|\lambda_\epsilon| \geq c > 0$ holds, satisfy $\mathrm{Re}(\lambda_\epsilon) \leq -c < 0$ for ϵ sufficiently small. This implies that $A = w_{\epsilon,t^\epsilon} + \phi_{\epsilon,t^\epsilon}$ is linearly stable.

□

Now we investigate the small eigenvalues of the problem (12.1), (12.2), i.e. we assume that $\lambda_\epsilon \to 0$ as $\epsilon \to 0$.

For ϵ small enough, let

$$\bar{w}_\epsilon = \xi_\epsilon^{-1}\left[w_{\epsilon,t^\epsilon} + \phi_{\epsilon,t^\epsilon}\right], \quad \bar{h}_\epsilon = T[w_{\epsilon,t^\epsilon} + \phi_{\epsilon,t^\epsilon}], \tag{12.6}$$

where t^ϵ is the point which has been determined by Liapunov-Schmidt reduction.

After re-scaling, the eigenvalue problem (12.1), (12.2) becomes

$$\begin{cases} \epsilon^2\Delta\phi_\epsilon - \phi_\epsilon + 2\dfrac{\bar{w}_\epsilon}{\bar{h}_\epsilon}\phi_\epsilon - \dfrac{\bar{w}_\epsilon^2}{\bar{h}_\epsilon^2}\psi_\epsilon = \lambda_\epsilon\phi_\epsilon, \\ (D(x)\psi_{\epsilon,x})_x - \psi_\epsilon + 2\xi_\epsilon\bar{w}_\epsilon\phi_\epsilon = \lambda_\epsilon\tau\psi_\epsilon, \end{cases} \tag{12.7}$$

where $\xi_\epsilon = \frac{1}{6\epsilon}$ is given by (4.8).

Our basic idea is the following: the eigenfunction ϕ_ϵ can be represented as

$$a_0^\epsilon \frac{d}{dt}(w_{\epsilon,t})\bigg|_{t=t^\epsilon}.$$

However, there is the following difficulty: note that $w_{\epsilon,t} \sim \xi_0(t)w\left(\frac{x-t}{\epsilon}\right)\chi\left(\frac{x-t}{r_0}\right)$. So when we differentiate $w_{\epsilon,t}$ with respect to t, we also need to differentiate $\xi_0(t)$ with respect to t.

Let us define

$$\tilde{w}_{\epsilon,0}(x) = \chi\left(\frac{x-t^\epsilon}{r_0}\right)\bar{w}_\epsilon(x), \tag{12.8}$$

where r_0 and $\chi(x)$ are given in (4.2) and (4.3) respectively. Similar to Appendix C, we define

$$\mathcal{K}_{\epsilon,t^\epsilon}^{new} := \text{span}\,\{\tilde{w}_{\epsilon,0}'\} \subset H^2(\Omega_\epsilon),$$

$$\mathcal{C}_{\epsilon,t^\epsilon}^{new} := \text{span}\,\{\tilde{w}_{\epsilon,0}'\} \subset L^2(\Omega_\epsilon).$$

Then it is easy to see that

$$\bar{w}_\epsilon(x) = \tilde{w}_{\epsilon,0}(x) + \text{e.s.t.} \tag{12.9}$$

and

$$\bar{h}_\epsilon'(t_0) = -\xi_\epsilon\int_{-1}^1 \nabla_{t_0}H(t_0,z)\bar{w}_\epsilon^2\,dz$$

$$= -[\nabla_x H(x,t_0)|_{x=t_0}]\hat{\xi}_0^2 + O(\epsilon) = O(\epsilon) \tag{12.10}$$

by (11.7).

Note that $\tilde{w}_{\epsilon,0}(x) = \hat{\xi}_0 \tilde{w}_0(x) + O(\epsilon)$ in $H^2_\epsilon(-1,1)$ and $\tilde{w}_{\epsilon,0}$ satisfies

$$\epsilon^2 \Delta \tilde{w}_{\epsilon,0} - \tilde{w}_{\epsilon,0} + \frac{(\tilde{w}_{\epsilon,0})^2}{\bar{h}_\epsilon} + \text{e.s.t.} = 0.$$

Thus $\tilde{w}^{'}_{\epsilon,0} := \frac{d\tilde{w}_{\epsilon,0}}{dx}$ satisfies

$$\epsilon^2 \Delta \tilde{w}^{'}_{\epsilon,0} - \tilde{w}^{'}_{\epsilon,0} + \frac{2\tilde{w}_{\epsilon,0}}{\bar{h}_\epsilon} \tilde{w}^{'}_{\epsilon,0} - \frac{\tilde{w}^2_{\epsilon,0}}{(\bar{h}_\epsilon)^2} \bar{h}^{'}_\epsilon + \text{e.s.t.} = 0. \tag{12.11}$$

Let us now decompose

$$\phi_\epsilon = \epsilon a^\epsilon_0 \tilde{w}^{'}_{\epsilon,0} + \phi^\perp_\epsilon \tag{12.12}$$

with complex numbers a^ϵ_0. (The scaling factor ϵ is introduced to ensure $\phi_\epsilon = O(1)$ in $H^2(\Omega_\epsilon)$), where $\phi^\perp_\epsilon \perp \mathcal{K}^{new}_{\epsilon,t^\epsilon}$.

Suppose that $\|\phi_\epsilon\|_{H^2(\Omega_\epsilon)} = 1$. Then $|a^\epsilon_j| \le C$.

The decomposition of ϕ_ϵ implies the following decomposition of ψ_ϵ:

$$\psi_\epsilon = \epsilon a^\epsilon_0 \psi_{\epsilon,0} + \psi^\perp_\epsilon, \quad \psi_{\epsilon,0},\, \psi^\perp_\epsilon \in H^2_N(\Omega_\epsilon) \tag{12.13}$$

where $\psi_{\epsilon,0}$ satisfies

$$(D(x)\psi_{\epsilon,0,x})_x - \psi_{\epsilon,0} + 2\xi_\epsilon \bar{w}_\epsilon \tilde{w}^{'}_{\epsilon,0} = 0 \tag{12.14}$$

and $\psi^\perp_\epsilon$ is given by

$$(D(x)\psi^\perp_{\epsilon,x})_x - \psi^\perp_\epsilon + 2\xi_\epsilon \bar{w}_\epsilon \phi^\perp_\epsilon = 0. \tag{12.15}$$

Substituting the decompositions of ϕ_ϵ and ψ_ϵ into (12.7), we have, using (12.11),

$$\begin{aligned} &\epsilon a^\epsilon_0 \left(\frac{(\tilde{w}_{\epsilon,0})^2}{\bar{h}^2_\epsilon} \bar{h}^{'}_\epsilon - \frac{(\bar{w}_\epsilon)^2}{\bar{h}^2_\epsilon} \psi_{\epsilon,0} \right) \\ +\epsilon^2 \Delta \phi^\perp_\epsilon - \phi^\perp_\epsilon + 2\frac{\bar{w}_\epsilon}{\bar{h}_\epsilon} \phi^\perp_\epsilon - \frac{\bar{w}^2_\epsilon}{\bar{h}^2_\epsilon} \psi^\perp_\epsilon - \lambda_\epsilon \phi^\perp_\epsilon + \text{e.s.t.} \quad &= \quad \lambda_\epsilon \epsilon a^\epsilon_0 \tilde{w}^{'}_{\epsilon,0}. \end{aligned} \tag{12.16}$$

Let us first compute

$$\begin{aligned} I_4 \quad &:= \quad \epsilon a^\epsilon_0 \left(\frac{(\tilde{w}_{\epsilon,0})^2}{\bar{h}^2_\epsilon} \bar{h}^{'}_\epsilon - \frac{(\bar{w}_\epsilon)^2}{\bar{h}^2_\epsilon} \psi_{\epsilon,0} \right) \\ &= \quad \epsilon a^\epsilon_0 \frac{(\tilde{w}_{\epsilon,0})^2}{\bar{h}^2_\epsilon} \left[-\psi_{\epsilon,0} + \bar{h}^{'}_\epsilon \right] + \text{e.s.t.}. \end{aligned}$$

Let us also put

$$\tilde{L}_\epsilon \phi^\perp_\epsilon := \epsilon^2 \Delta \phi^\perp_\epsilon - \phi^\perp_\epsilon + \frac{2\bar{w}_\epsilon}{\bar{h}_\epsilon} \phi^\perp_\epsilon - \frac{\bar{w}^2_\epsilon}{\bar{h}^2_\epsilon} \psi^\perp_\epsilon. \tag{12.17}$$

Multiplying both sides of (12.16) by $\tilde{w}_{\epsilon,0}^{'}$ and integrating over $(-1,1)$, we obtain

$$\begin{aligned} \text{r.h.s.} &= \epsilon\lambda_\epsilon a_0^\epsilon \int_{-1}^{1} \tilde{w}_{\epsilon,0}^{'}\tilde{w}_{\epsilon,0}^{'}\,dx \\ &= \lambda_\epsilon a_0^\epsilon \hat{\xi}_0^2 \int_R (w^{'}(y))^2\,dy\ (1+O(\epsilon)) \end{aligned} \tag{12.18}$$

and

$$\begin{aligned} \text{l.h.s.} &= -\epsilon a_0^\epsilon \int_{-1}^{1} \frac{\tilde{w}_{\epsilon,0}^2}{\bar{h}_\epsilon^2}\left[\psi_{\epsilon,0}-\bar{h}_\epsilon^{'}\right]\tilde{w}_{\epsilon,0}^{'}\,dx + \int_{-1}^{1}\frac{\tilde{w}_{\epsilon,0}^2}{\bar{h}_\epsilon^2}(\bar{h}_\epsilon^{'}\phi_\epsilon^\perp)\,dx - \int_{-1}^{1}\frac{\tilde{w}_{\epsilon,0}^2}{\bar{h}_\epsilon^2}(\psi_\epsilon^\perp\tilde{w}_{\epsilon,0}^{'})\,dx \\ &= (J_1+J_2+J_3)(1+O(\epsilon)) \quad \text{by (12.11)}, \end{aligned}$$

where J_i, $i=1,2,3$, are defined by the last equality.

For J_3, we decompose

$$J_3 = J_4 + J_5,$$

where

$$J_4 = -\int_{-1}^{1}\frac{\tilde{w}_{\epsilon,0}^2}{\bar{h}_\epsilon^2}(\psi_\epsilon^\perp(t^\epsilon)\tilde{w}_{\epsilon,0}^{'})\,dx \tag{12.19}$$

$$J_5 = -\int_{-1}^{1}\frac{\tilde{w}_{\epsilon,0}^2}{\bar{h}_\epsilon^2}(\psi_\epsilon^\perp(x)-\psi_\epsilon^\perp(t^\epsilon))\tilde{w}_{\epsilon,0}^{'}\,dx. \tag{12.20}$$

The following is the key lemma.

Lemma 12.2. *We have*

$$J_1 = -\epsilon^2\left(\frac{1}{3}\int_R w^3\,dy\right)\hat{\xi}_0^3\left(\nabla_{t^\epsilon}^2 H(t^\epsilon,t^\epsilon)\right)a_0^\epsilon + o(\epsilon^2), \tag{12.21}$$

$$J_2+J_3 = o(\epsilon^2). \tag{12.22}$$

Proof: Lemma 12.2 follows from the following series of lemmas. We first study the asymptotic behavior of $\psi_{\epsilon,0}$.

Lemma 12.3. *We have*

$$(\psi_{\epsilon,0}-\bar{h}_\epsilon^{'})(t^\epsilon) = \hat{\xi}_0^2\nabla_{t^\epsilon}H(t^\epsilon,t^\epsilon)+O(\epsilon). \tag{12.23}$$

Proof: We compute $\psi_{\epsilon,0}-\bar{h}_\epsilon'$ near t^ϵ:

$$\begin{aligned}\bar{h}_\epsilon(x) &= \xi_\epsilon\int_{-1}^{1}G(x,z)\bar{w}_\epsilon^2\,dz\\ &= \xi_\epsilon\int_{-\infty}^{+\infty}K_D(|z|)\tilde{w}_{\epsilon,0}^2(x+z)dz-\xi_\epsilon\int_{-1}^{1}H(x,z)\tilde{w}_{\epsilon,0}^2\,dz+O(\epsilon).\end{aligned}$$

So

$$\bar{h}_\epsilon'(x) = \xi_\epsilon\int_{-\infty}^{+\infty}K_D(|z|)(2\tilde{w}_{\epsilon,0}(x+z)\tilde{w}_{\epsilon,0}'(x+z))\,dz-\xi_\epsilon\int_{-1}^{1}\nabla_xH(x,z)\tilde{w}_{\epsilon,0}^2\,dz+O(\epsilon).$$

Thus

$$(\bar{h}_\epsilon'-\psi_{\epsilon,0})(x) = -\xi_\epsilon\int_{-1}^{1}\nabla_xH(x,z)\tilde{w}_{\epsilon,0}^2(z)\,dz-\left(-2\xi_\epsilon\int_{-1}^{1}H(x,z)\tilde{w}_{\epsilon,0}\tilde{w}_{\epsilon,0}'\,dz\right)+O(\epsilon).$$

Therefore,

$$\begin{aligned}(\bar{h}_\epsilon'-\psi_{\epsilon,0})(t^\epsilon) &= -\xi_\epsilon\int_{-1}^{1}\nabla_{t^\epsilon}H(t^\epsilon,z)\tilde{w}_{\epsilon,0}^2(z)\,dz-\nabla_z|_{z=t^\epsilon}H(t^\epsilon,z)\hat{\xi}_0^2+O(\epsilon)\\ &= -\nabla_z|_{z=t^\epsilon}H(z,t^\epsilon)\hat{\xi}_0^2-\nabla_z|_{z=t^\epsilon}H(t^\epsilon,z)\hat{\xi}_0^2+O(\epsilon).\\ &= -\nabla_{t^\epsilon}H(t^\epsilon,t^\epsilon)\hat{\xi}_0^2+O(\epsilon). \qquad (12.24)\end{aligned}$$

This implies (12.23).

□

Similar to the proof of Lemma 12.3, the following result is derived.

Lemma 12.4. *We have*

$$(\psi_{\epsilon,0}-\bar{h}_\epsilon')(t^\epsilon+\epsilon y)-(\psi_{\epsilon,0}-\bar{h}_\epsilon')(t^\epsilon) \qquad (12.25)$$

$$=\epsilon y\nabla_{t^\epsilon}^2H(t^\epsilon,t^\epsilon)\hat{\xi}_0^2+O(\epsilon^2y^2).$$

Next we estimate $\phi_\epsilon^\perp$. We derive

Lemma 12.5. *For ϵ sufficiently small, we have*

$$\|\phi_\epsilon^\perp\|_{H^2(\Omega_\epsilon)}=O(\epsilon^2). \qquad (12.26)$$

Proof: As the first step in the proof of Lemma 12.5, we obtain a relation between $\psi_\epsilon^\perp$ and $\phi_\epsilon^\perp$. Note that similar to the proof of Proposition 10.1, $\tilde{L}_\epsilon$ is invertible from $(\mathcal{K}_\epsilon^{new})^\perp$ to $(\mathcal{C}_\epsilon^{new})^\perp$ with uniformly bounded inverse for ϵ small enough. By (12.16), Lemma 12.3 and the fact that $\tilde{L}_\epsilon$ is uniformly invertible, we deduce that

$$\|\phi_\epsilon^\perp\|_{H^2(\Omega_\epsilon)} = O(\epsilon). \tag{12.27}$$

Let us cut off

$$\tilde{\phi}_{\epsilon,0} = \frac{\phi_\epsilon^\perp}{\epsilon}\chi\left(\frac{x-t^\epsilon}{r_0}\right). \tag{12.28}$$

Then

$$\phi_\epsilon^\perp = \epsilon\tilde{\phi}_{\epsilon,0} + O(\epsilon^2).$$

Suppose that

$$\tilde{\phi}_{\epsilon,0} \to \phi_0 \ \text{ in } H^2_{N,loc}(\Omega_\epsilon). \tag{12.29}$$

Then we have by the equation for $\psi_\epsilon^\perp$:

$$\begin{aligned}\psi_\epsilon^\perp(t^\epsilon) &= 2\epsilon\xi_\epsilon\int_{-1}^{1} G(t^\epsilon,z)\bar{w}_\epsilon\tilde{\phi}_{\epsilon,0}\,dz \\ &= 2\epsilon G(t^\epsilon,t^\epsilon)\hat{\xi}_0\frac{\int_R w\phi_0\,dy}{\int_R w^2\,dy} + O(\epsilon^2).\end{aligned} \tag{12.30}$$

This relation between $\psi_\epsilon^\perp$ and $\phi_\epsilon^\perp$ will be important for the rest of the proof.

Now we substitute (12.30) into (12.16) and, using Lemma 12.3, we have that the limit ϕ_0 satisfies

$$\Delta\phi_0 - \phi_0 + 2w\phi_0 - 2G(t_0,t_0)\hat{\xi}_0\frac{\int_R w\phi_0}{\int_R w^2}w^2 + \nabla_{t_0}H(t_0,t_0)\hat{\xi}_0^2 a^0 w^2 = 0, \tag{12.31}$$

where

$$a^0 = \lim_{\epsilon\to 0} a_\epsilon.$$

Hence, using the relations

$$G(t_0,t_0)\hat{\xi}_0 = 1, \quad \nabla_{t_0}H(t_0,t_0) = 0,$$

we can apply Theorem 2.1 (3) with $\gamma = 2$, which implies that $\phi_0 = 0$.

Finally, we deduce

$$\phi_\epsilon^\perp = \epsilon\tilde{\phi}_{\epsilon,0} + O(\epsilon^2) = \epsilon\phi_0\left(\frac{x-t^\epsilon}{\epsilon}\right) + O(\epsilon^2) = O(\epsilon^2), \tag{12.32}$$

which implies (12.26).

□

By (12.32), we have $J_2 = o(\epsilon^2)$.

From Lemma 12.5 and (12.30), we have that

$$\psi_\epsilon^\perp(t^\epsilon) = O(\epsilon^2). \tag{12.33}$$

Further,

$$\psi_\epsilon^\perp(t^\epsilon+\epsilon y) - \psi_\epsilon^\perp(t^\epsilon) \;=\; -2\epsilon^2 y \nabla_{t^\epsilon} H(t^\epsilon,t^\epsilon)\hat{\xi}_0 \frac{\int_R w\phi_0\,dy}{\int_R w^2\,dy} + O(\epsilon^3) = O(\epsilon^3). \tag{12.34}$$

This implies $J_4 = o(\epsilon^2)$ and $J_5 = o(\epsilon^2)$.

The computation of J_1 follows from Lemmas 12.3 and 12.4. In fact,

$$\begin{aligned} J_1 &= -\epsilon a_0^\epsilon \int_{-1}^1 \frac{\tilde{w}_{\epsilon,0}^2}{\bar{h}_\epsilon^2}\left(\psi_{\epsilon,0} - \bar{h}_\epsilon'\right)\tilde{w}_{\epsilon,0}'\,dx + o(\epsilon^2) \\ &= -\epsilon a_0^\epsilon \int_{-1}^1 \frac{\tilde{w}_{\epsilon,0}^2}{\bar{h}_\epsilon^2}\left(\psi_{\epsilon,0}(t_0) - \bar{h}_\epsilon'(t_0)\right)\tilde{w}_{\epsilon,0}'\,dx + o(\epsilon^2) \\ &\quad -\epsilon a_0^\epsilon \int_{-1}^1 \frac{\tilde{w}_{\epsilon,0}^2}{\bar{h}_\epsilon^2}\left([\psi_{\epsilon,0}(x) - \bar{h}_\epsilon'(x)] - [\psi_{\epsilon,0}(t_0) - \bar{h}_\epsilon'(t_0)]\right)\tilde{w}_{\epsilon,0}'\,dx + o(\epsilon^2) \\ &= J_6 + J_7. \end{aligned}$$

For J_6, we use Lemma 12.3 to obtain

$$\begin{aligned} J_6 &= -\frac{2}{3}\epsilon a_0^\epsilon \int_{-1}^1 \frac{\tilde{w}_{\epsilon,0}^3}{\bar{h}_\epsilon^3}\bar{h}_\epsilon'\left(\psi_{\epsilon,0}(t_0) - \bar{h}_\epsilon'(t_0)\right)\,dx + o(\epsilon^2) \\ &= -\frac{2}{3}\epsilon^2 a_0^\epsilon \left(\int_R w^3\,dy\right)\bar{h}_\epsilon'(t^\epsilon)\hat{\xi}_0^2 \nabla_{t^\epsilon} H(t^\epsilon,t^\epsilon) + o(\epsilon^2) = o(\epsilon^2) \end{aligned} \tag{12.35}$$

since $\nabla_{t^\epsilon} H(t^\epsilon,t^\epsilon) = o(1)$. Finally, using Lemma 12.4, we compute the main contribution:

$$\begin{aligned} J_7 &= \epsilon^2 \hat{\xi}_0 \int_R \left(y w^2 w'(y)\right)\,dy \nabla_{t^\epsilon}^2 H(t^\epsilon,t^\epsilon)\hat{\xi}_0^2 a_0^\epsilon + o(\epsilon^2) \\ &= -\epsilon^2 \left(\frac{1}{3}\int_R w^3\,dy\right)\hat{\xi}_0^3 \nabla_{t^\epsilon}^2 H(t^\epsilon,t^\epsilon) a_0^\epsilon + o(\epsilon^2). \end{aligned} \tag{12.36}$$

Combining (12.35), (12.36) and using (12.10), Lemma 12.3, Lemma 12.4, we obtain (12.21).

This concludes the proof of Lemma 12.2.

□

Comparing (12.18) with (12.19) r.h.s. and using Lemma 12.2, (2.3), we obtain

$$-2.4\epsilon^2 \hat{\xi}_0^3 \left(\nabla_{t^\epsilon}^2 H(t^\epsilon,t^\epsilon)\right) a_0^\epsilon + o(\epsilon^2) = \lambda_\epsilon \hat{\xi}_0^2 a_0^\epsilon 1.2\,(1+o(1)). \tag{12.37}$$

Equation (12.37) implies that the small eigenvalue λ_ϵ of (12.7) satisfies

$$\lambda_\epsilon = -2\epsilon^2 \hat{\xi}_0 \left(\nabla_{t^\epsilon}^2 H(t^\epsilon,t^\epsilon)\right) + o(\epsilon^2).$$

Arguing as in Theorem 12.1, this shows that since by (8.7) $\nabla^2_{t^\epsilon} H(t^\epsilon, t^\epsilon)$ is positive, the small eigenvalue λ_ϵ satisfies $\text{Re}(\lambda_\epsilon) \le -c\epsilon^2$ for some $c > 0$ which is independent of ϵ.

This fact, together with the results in the previous section, concludes the proof of Theorem 3.3.

□

13. Acknowledgments

The work of JW is supported by a grant of RGC of Hong Kong. The work of MW is supported by a BRIEF Award of Brunel University. MW thanks the Department of Mathematics at CUHK for their kind hospitality. We thank Karen Page for a very interesting discussion on biological modeling.

References

[1] D. L. Benson, P. K. Maini and J. A. Sherratt, Analysis of pattern formation in reaction diffusion models with spatially inhomogeneous diffusion coefficients, *Math. Comp. Mod.* 17 (1993), 29-34.

[2] D. L. Benson, P. K. Maini and J. A. Sherratt, Unravelling the Turing bifurcation using spatially varying diffusion coefficients, *J. Math. Biol.* 37 (1998), 381-387.

[3] D. L. Benson, J. A. Sherratt and P. K. Maini, Diffusion driven instability in an inhomogeneous domain, *Bull. Math. Biol.* 55 (1993), 365-384.

[4] S. S. Blair, Limb development: Marginal fringe benefits, *Current Biology* 7 (1997), R686-R690.

[5] S. S. Blair, Developmental biology: Notching the hindbrain, *Current Biology* 14 (2004), R570-R572.

[6] A.H. Boozer, Equations for studies of feedback stabilization, *Phys. Plasmas* 5 (1998), 3350.

[7] E.N. Dancer, On stability and Hopf bifurcations for chemotaxis systems, *Methods Appl. Anal.* 8 (2001), 245-256.

[8] A. Gierer and H. Meinhardt, A theory of biological pattern formation, *Kybernetik (Berlin)* 12 (1972), 30-39.

[9] D. Iron, M. J. Ward and J. Wei, The stability of spike solutions to the one-dimensional Gierer-Meinhardt model, *Physica D* 150 (2001), 25-62.

[10] K. D. Irvine and C. Rauskolb, Boundaries in development: Formation and function, *Annu. Rev. Cell Dev. Biol.* 17 (2001), 189-214.

[11] P. K. Maini, D. L. Benson and J. A. Sherratt, Pattern formation in reaction-diffusion models with spatially inhomogeneous diffusion coefficients, *IMA J. Math. Appl. Med. Biol.* 9 (1992), 197-213.

[12] H. Meinhardt, Cell determination boundaries as organizing regions for secondary embryonic fields, *Developmental Biology* 96 (1983), 375-385.

[13] I. Mercader, M. Net and E. Knobloch, Binary fluid convection in a cylinder, *Phys. Rev. E* 51 (1995), 339-350.

[14] J. Murray, Mathematical Biology I/II, Springer, 2002.

[15] Y. Nishiura, T. Teramoto, X. Yuan and K.-I. Ueda, Dynamics of traveling pulses in heterogeneous media, *Chaos* 17, (2007), 037104.

[16] K. Page, P. K. Maini and N. A. M. Monk, Pattern formation in spatially heterogeneous Turing reaction-diffusion models, *Phys. D* 181 (2003), 80-101.

[17] K. Page, P. K. Maini and N. A. M. Monk, Complex pattern formation in reaction-diffusion systems with spatially varying parameters, *Phys. D* 202 (2005), 95-115.

[18] A. M. Turing, The chemical basis of morphogenesis, *Phil. Trans. Roy. Soc. Lond. B* 237 (1952), 37-72.

[19] M. Ward, D. McInerney, P. Houston, D. Gavaghan and P. Maini, The dynamics and pinning of a spike for a reaction-diffusion system, *SIAM J. Appl. Math.* 62 (2002), 1297-1328.

[20] M.J. Ward and J. Wei, Hopf bifurcations and oscillatory instabilities of solutions for the one-dimensional Gierer-Meinhardt model, *J. Nonlinear Sci.* 13 (2003), 209-264.

[21] J. Wei, On single interior spike solutions of Gierer-Meinhardt system: uniqueness and spectrum estimates, *European J. Appl. Math.* 10 (1999), 353-378.

[22] J. Wei and M. Winter, On the two-dimensional Gierer-Meinhardt system with strong coupling, *SIAM J. Math. Anal.* 30 (1999), 1241-1263.

[23] J. Wei and M. Winter, Spikes for the two-dimensional Gierer-Meinhardt system: The strong coupling case, *J. Differential Equations* 178 (2000), 478-518.

[24] J. Wei and M. Winter, Spikes for the two-dimensional Gierer-Meinhardt system: The weak coupling case, *J. Nonlinear Science* 11 (2001), 415-458.

[25] J. Wei and M. Winter, On the Gierer-Meinhardt System with Precursors, *Discrete Contin. Dyn. Syst. Ser. A*, to appear.

[26] L. Wolpert, Positional information and the spatial pattern of cellular differentiation, *J. Theor. Biology* 25 (1969), 1-47.

[27] L. Wolpert and A. Hornbruch, Double anterior chick limb buds and models for cartilage rudiment specification, *Development* 109 (1990), 961-966.

Department of Mathematics, The Chinese University of Hong Kong, Shatin, Hong Kong
E-mail address: wei@math.cuhk.edu.hk

Brunel University, Department of Mathematical Sciences, Uxbridge, UB8 3PH, United Kingdom
E-mail address: matthias.winter@brunel.ac.uk